Hadron Collider Physics Symposium 2011

Soft Physics at RHIC

Michal Šumbera

Nuclear Physics Institute AS CR, Řež/Prague

(for the STAR and PHENIX Collaborations)

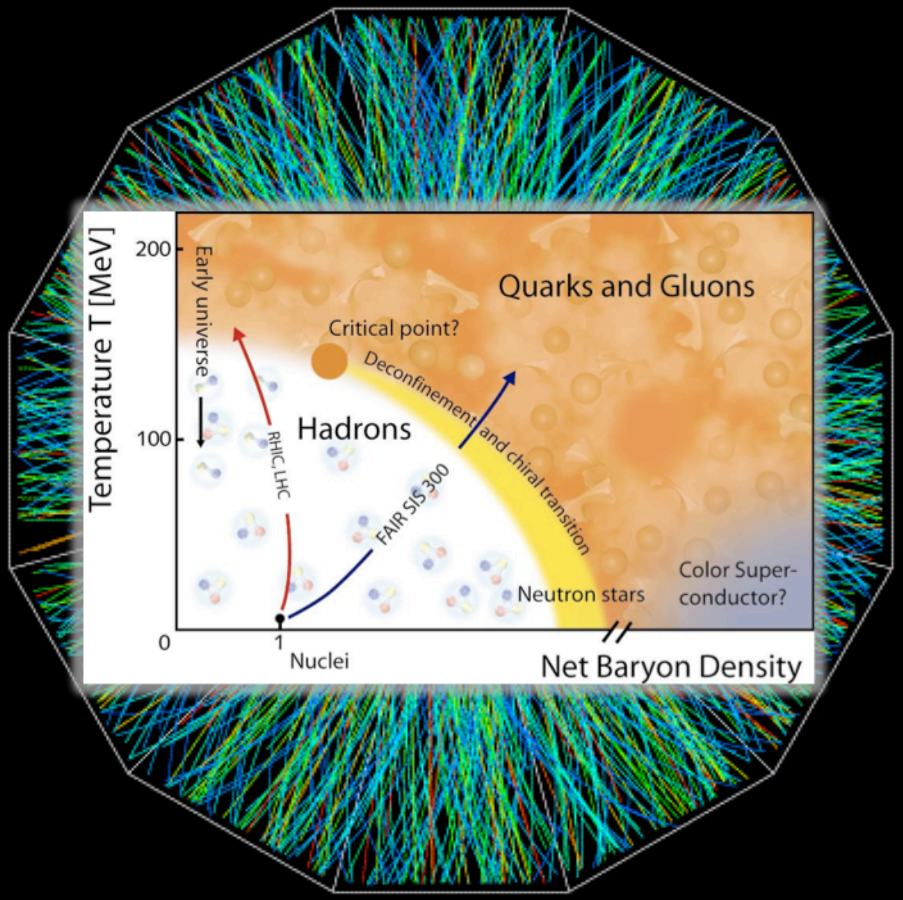

Remarkable discoveries at RHIC

- Perfect liquid BRAHMS, PHENIX, PHOBOS, STAR, Nuclear Physics A757 (2005)1-283
- Number of constituent quark scaling

  PHENIX, PRL 91(2003)072301; STAR, PR C70(2005) 014904
- Jet quenching PHENIX, PRL 88(2002)022301; STAR, PRL 90(2003) 082302
- Heavy-quark suppression PHENIX, PRL 98(2007)172301,
  STAR, PRL 98(2007)192301
- Production of exotic systems
  - Discovery on anti-strange nucleus STAR, Science 328 (2010) 58
  - Observation of anti-^{4}He nucleus STAR, Nature 473 (2011) 353
- Indications of gluon saturation at small x STAR, PRL 90(2003) 082302; BRAHMS, PRL 91(2003) 072305; PHENIX ibid 072303

Remarkable discoveries at RHIC

- Perfect liquid BRAHMS, PHENIX, PHOBOS, STAR, Nuclear Physics A757 (2005)1-283
- Number of constituent quark scaling

  PHENIX, PRL 91(2003)072301; STAR, PR C70(2005) 014904
- Jet quenching PHENIX, PRL 88(2002)022301; STAR, PRL 90(2003) 082302
- Heavy-quark suppression PHENIX, PRL 98(2007)172301, STAR, PRL 98(2007)192301
- Production of exotic systems
  - Discovery on anti-strange nucleus STAR, Science 328 (2010) 58
  - Observation of anti-^{4}He nucleus STAR, Nature 473 (2011) 353
- Indications of gluon saturation at small x STAR, PRL 90(2003) 082302; BRAHMS, PRL 91(2003) 072305; PHENIX ibid 072303

Relativistic Heavy Ion Collider (RHIC)

Brookhaven National Laboratory (BNL), Upton, NY

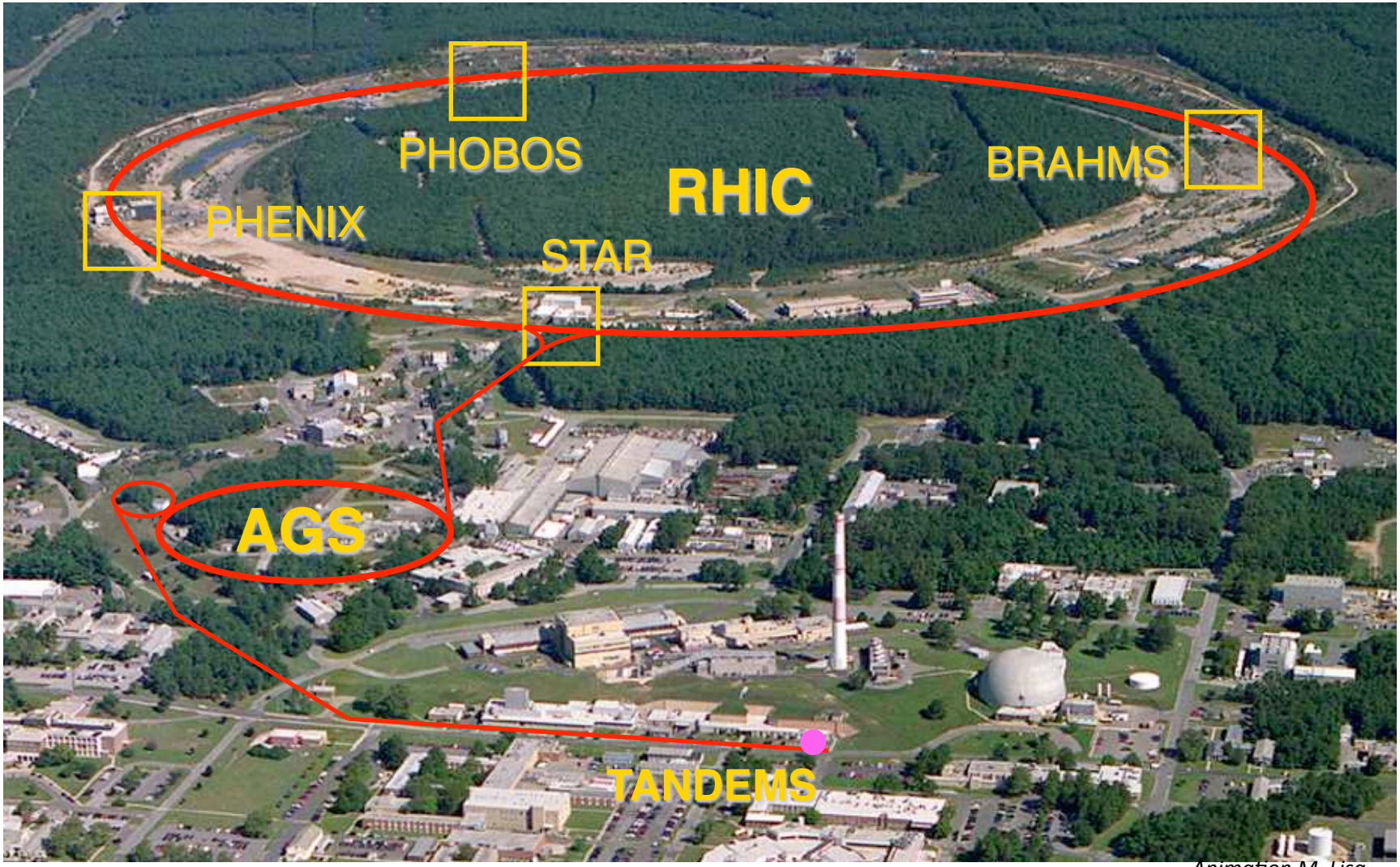

Animation M. Lisa

World's (second) largest operational heavy-ion collider

World's largest polarized proton collider

Relativistic Heavy Ion Collider (RHIC)

Brookhaven National Laboratory (BNL), Upton, NY

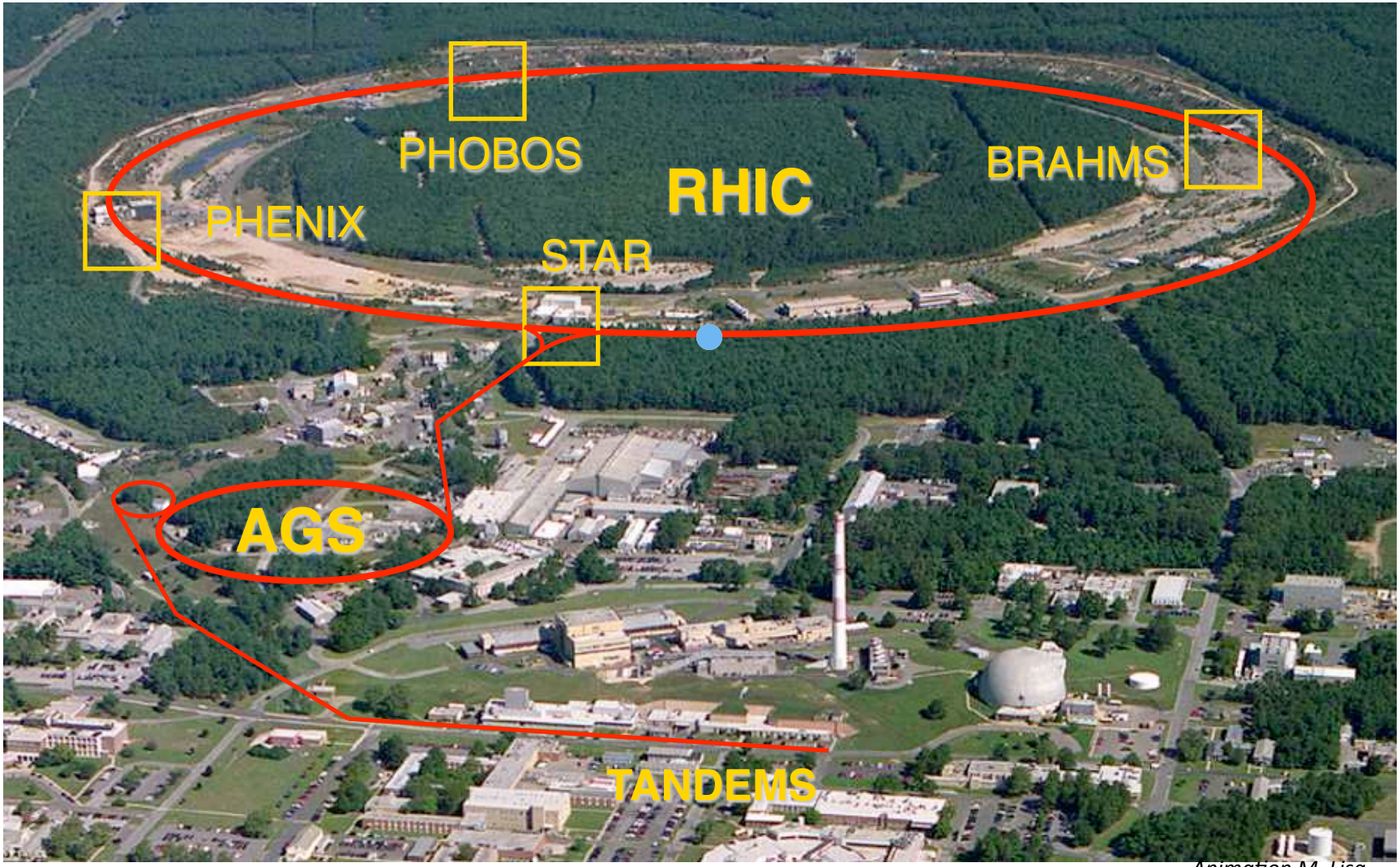

Animation M. Lisa

World's (second) largest operational heavy-ion collider

World's largest polarized proton collider

Relativisti r (RHIC)

Brook

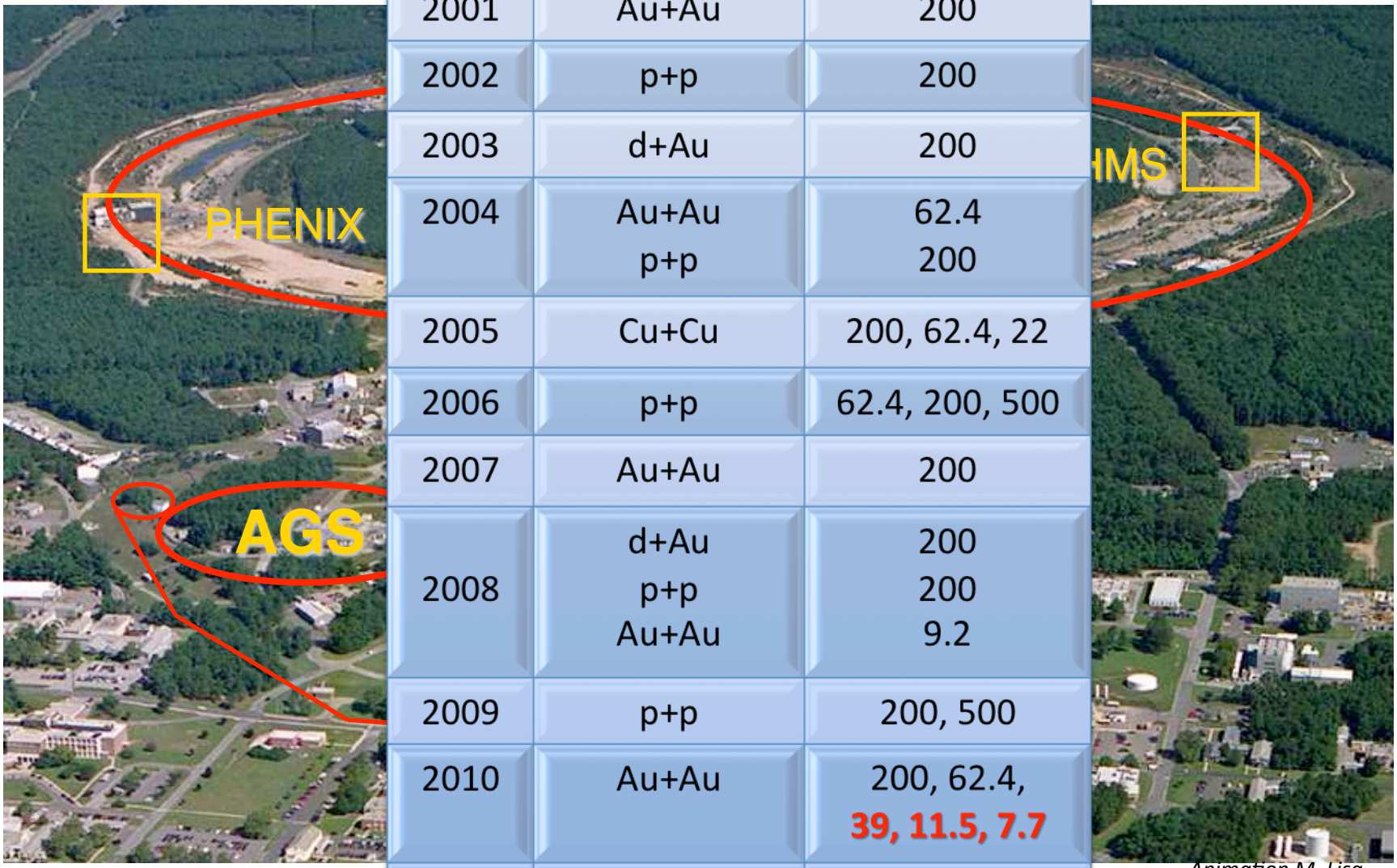

Year	System	$\sqrt{s_{NN}}$ [GeV]
2000	Au+Au	130
2001	Au+Au	200
2002	p+p	200
2003	d+Au	200
2004	Au+Au p+p	62.4 200
2005	Cu+Cu	200, 62.4, 22
2006	p+p	62.4, 200, 500
2007	Au+Au	200
2008	d+Au p+p Au+Au	200 200 9.2
2009	p+p	200, 500
2010	Au+Au	200, 62.4, **39, 11.5, 7.7**
2011	Au+Au p+p	200,19.6,27 500

Animation M. Lisa

World n collider

r

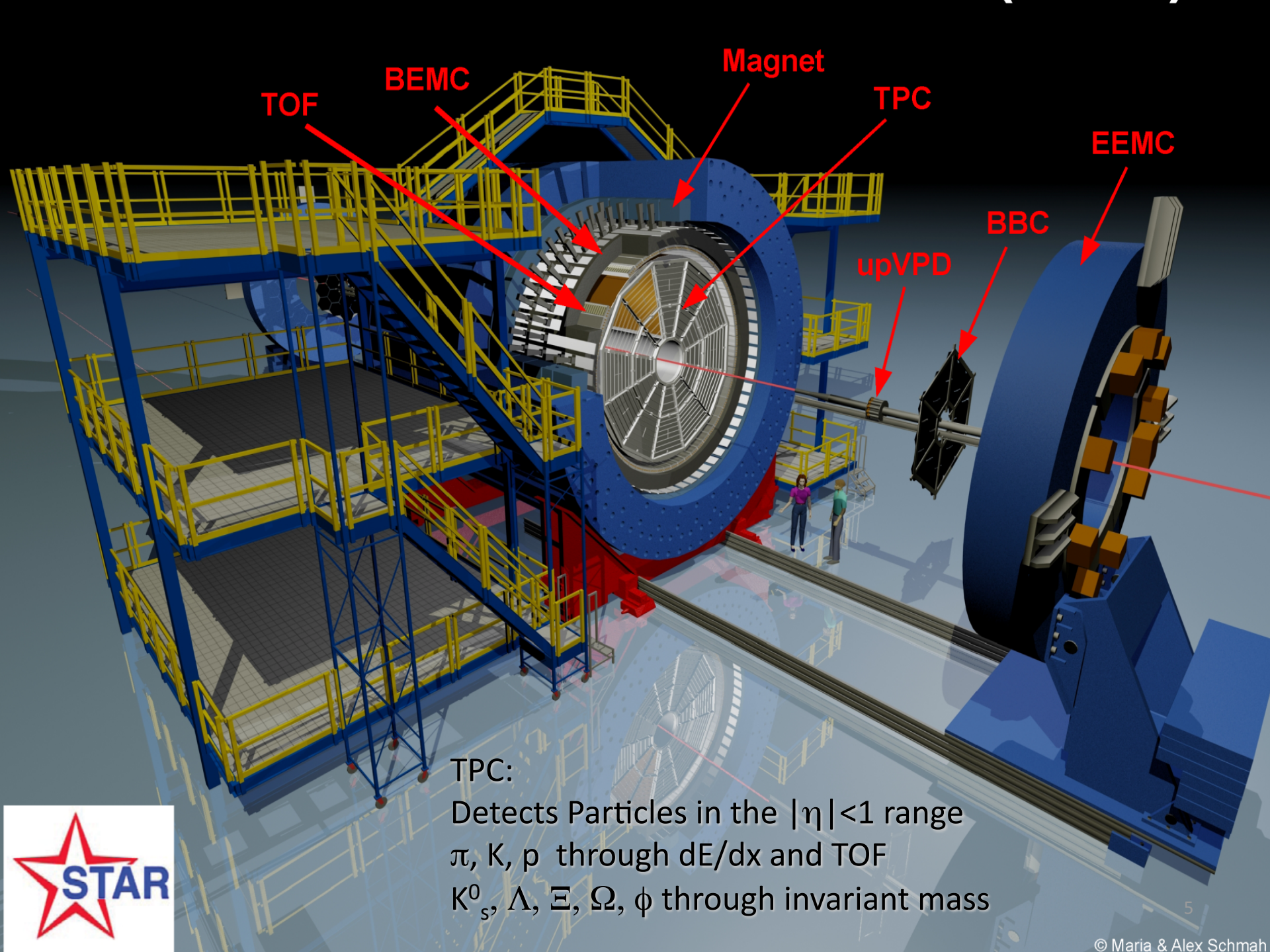

TPC:

Detects Particles in the $|\eta|<1$ range

π, K, p through dE/dx and TOF

K^0_s, Λ, Ξ, Ω, ϕ through invariant mass

Central Au+Au at 7.7 GeV in STAR TPC

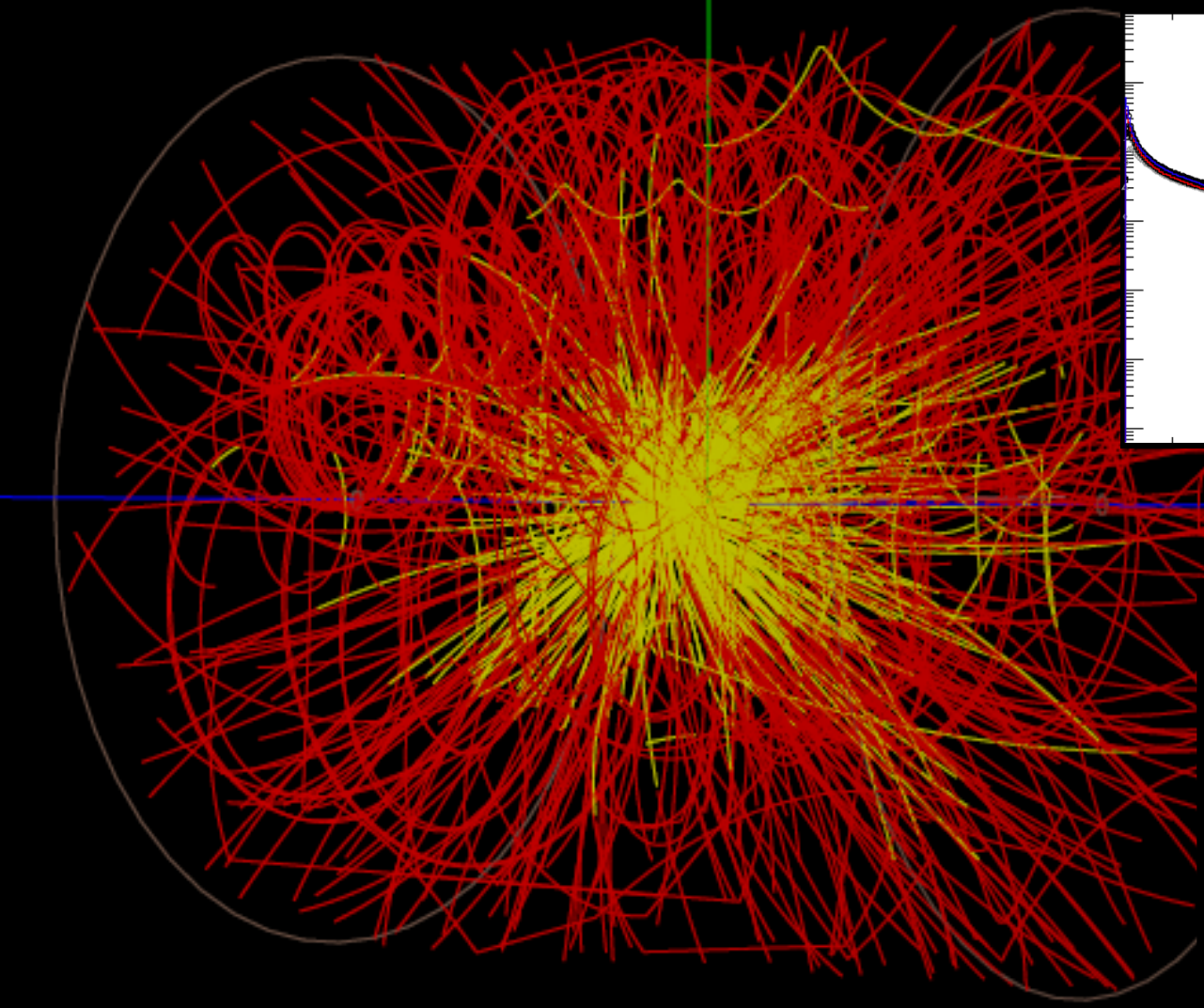

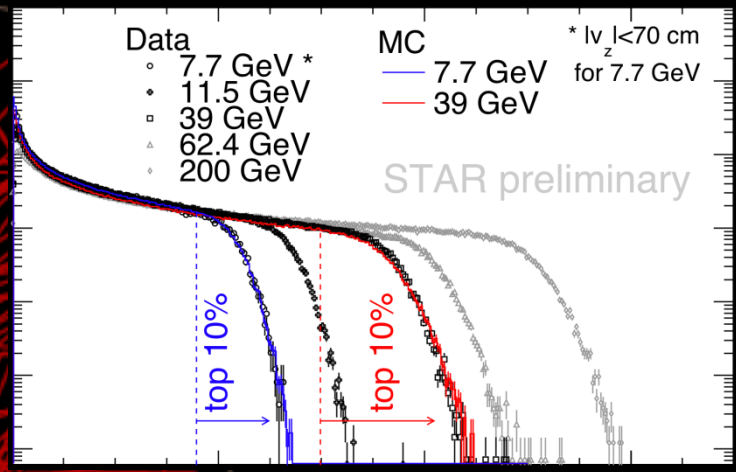

Detector performance generally improves at lower energies.

Geometric acceptance remains the same, track density gets lower. Triggering required effort, but was a solvable problem.

Au+Au @ 7.7 GeV

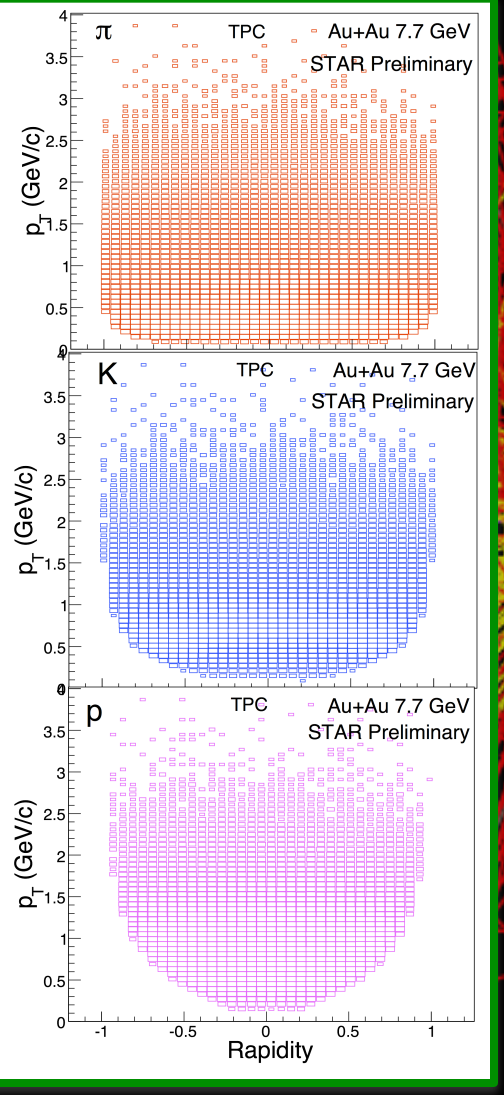

Au+Au @ 200 GeV

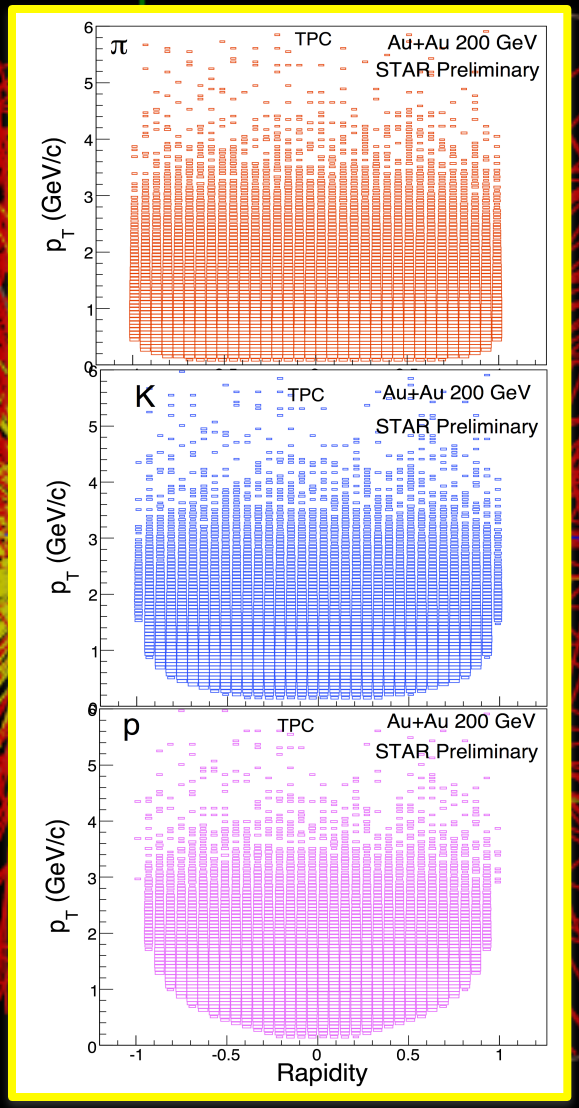

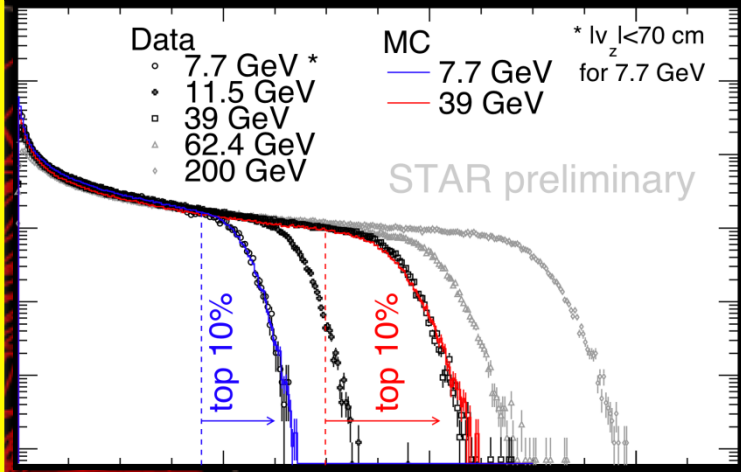

Detector performance generally improves at lower energies.

Geometric acceptance remains the same, track density gets lower. Triggering required effort, but was a solvable problem.

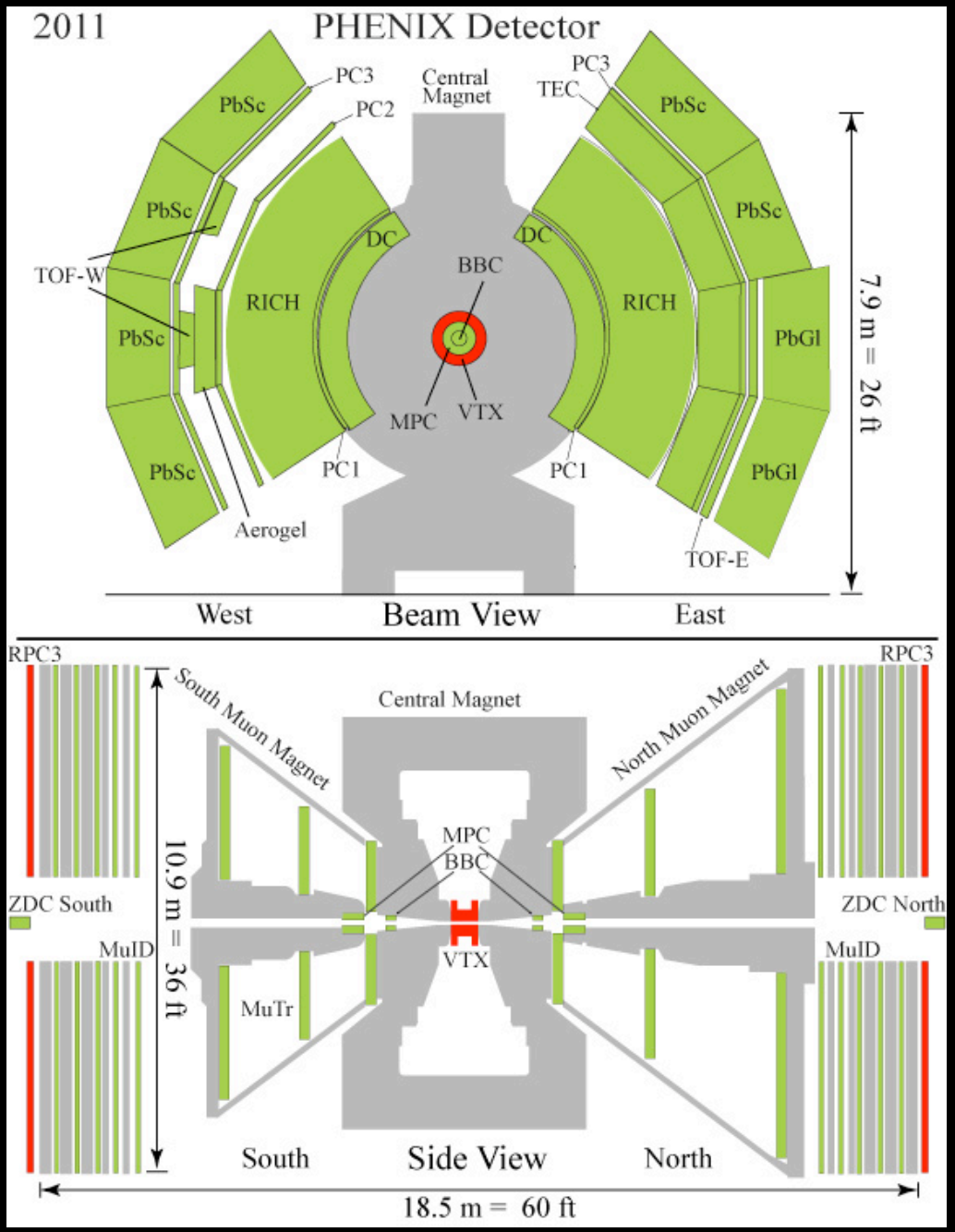

Central arms:

Hadrons, photons, electrons

- $J/\psi \rightarrow e^+e^-$; $\psi' \rightarrow e^+e^-$; $\chi_c \rightarrow e^+e^-\Upsilon$;
- $|\eta| < 0.35$
- $p_e > 0.2$ GeV/c
- $\Delta\phi = \pi$ (2 arms x $\pi/2$)

Forward rapidity arms:

Muons

- $J/\psi \rightarrow \mu^+\mu^-$; $\Upsilon \rightarrow \mu^+\mu^-$
- $1.2 < |\eta| < 2.2$
- $p_\mu > 1$ GeV/c
- $\Delta\varphi = 2\pi$

PHENIX

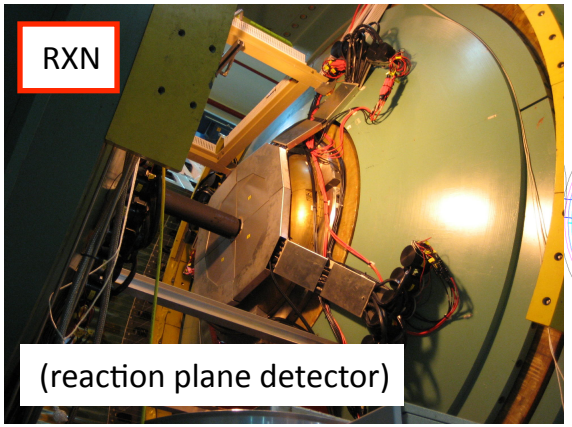

(reaction plane detector)

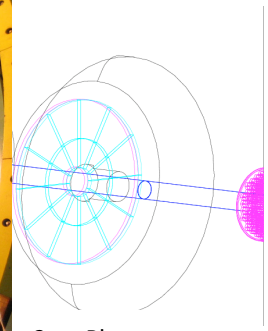

2cm Pb converter
in front

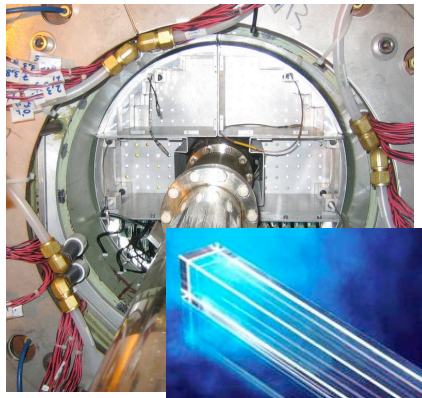

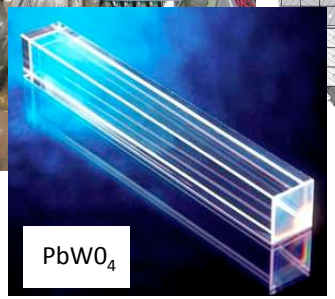

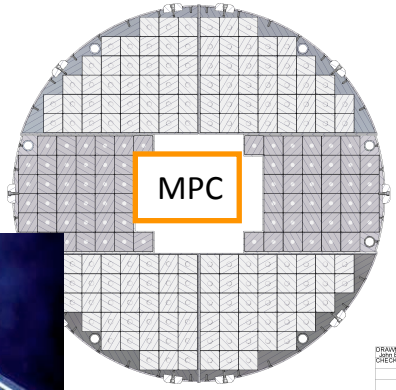

(muon piston
EM-calorimeter)

(zero degree n calorimeter
/shower max detector)

ZDC/SMD

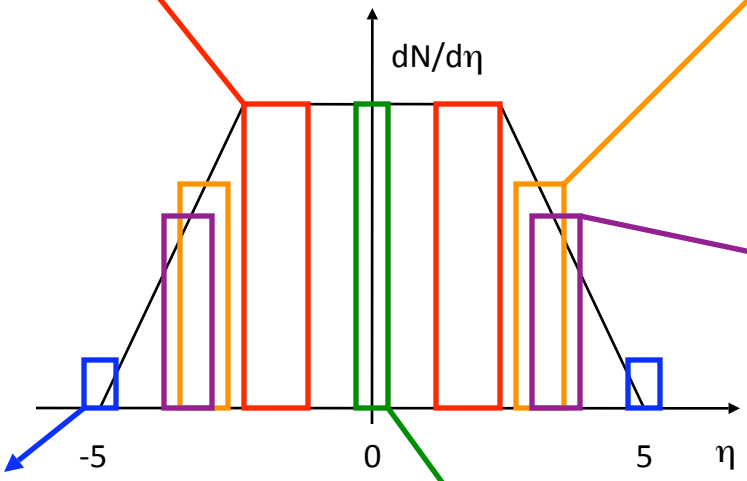

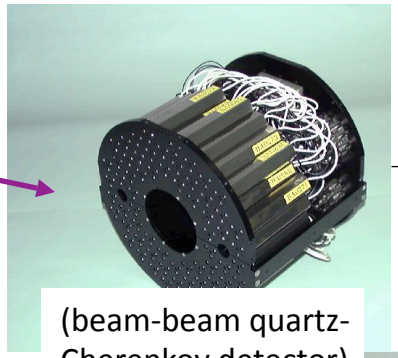

(beam-beam quartz-
Cherenkov detector)

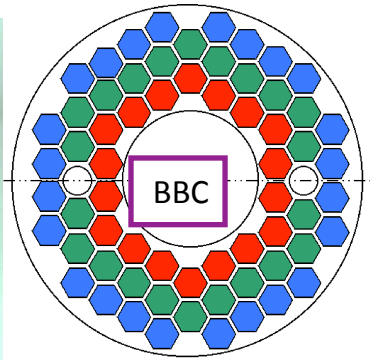

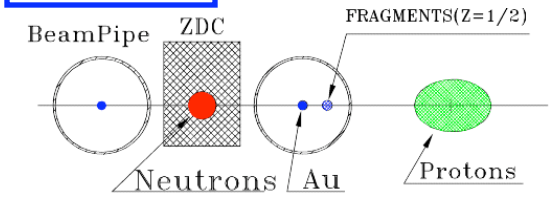

CNT

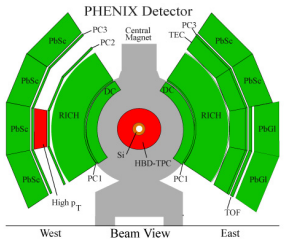

(PHENIX central tracking arm)

PHENIX

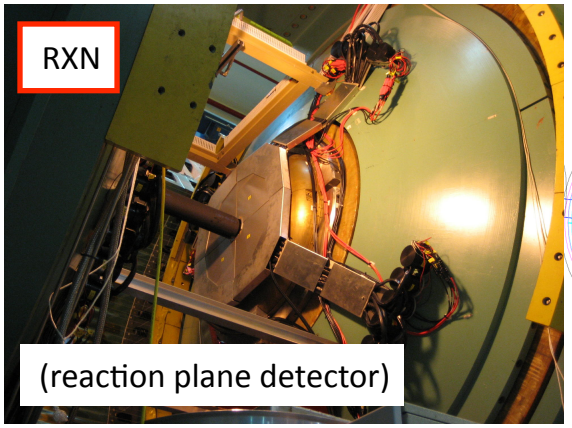

(reaction plane detector)

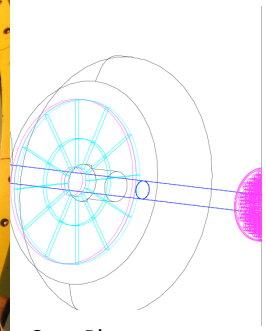

2cm Pb converter
in front

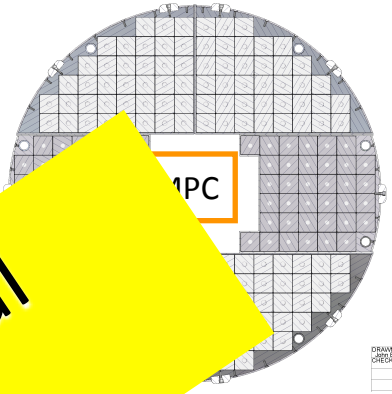

(muon piston
EM-calorimeter)

Wide range of η coverage with several R.P. detectors for systematic studies

ZDC/SMD

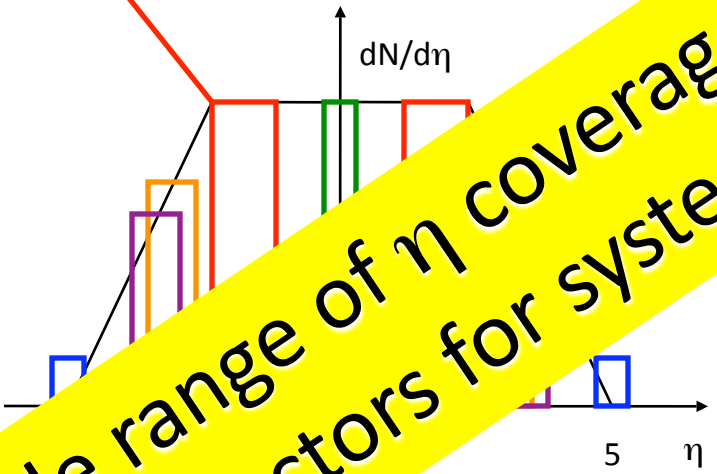

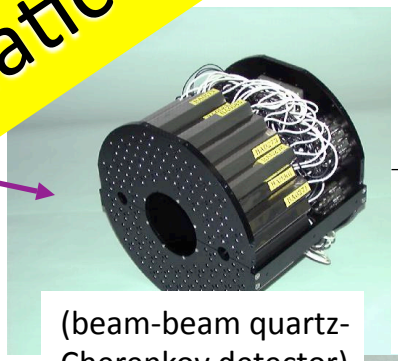

(beam-beam quartz-
Cherenkov detector)

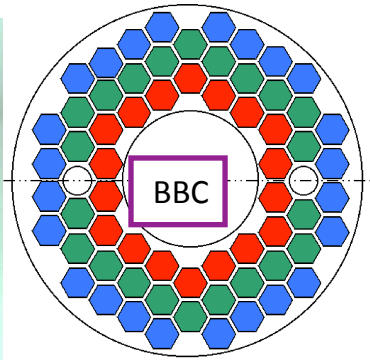

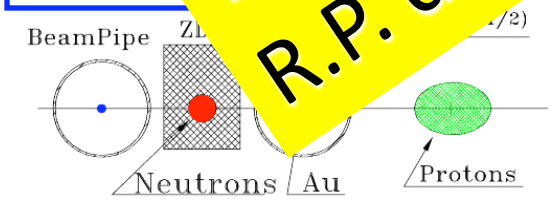

CNT

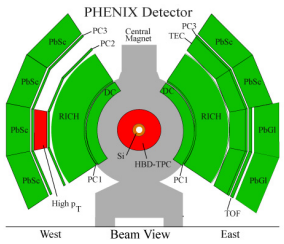

(PHENIX central tracking arm)

PHENIX

The RHIC Beam Energy Scan Program

- Lattice Gauge Theory (LGT) prediction on the transition temperature T_C is robust.
- LGT calculation, universality, and models hinted the existence of the critical point (CP) on the QCD phase diagram at finite μ_B.
- Experimental evidence for either the CP or 1st order transition is important for understanding the QCD phase diagram.

- In 2009 the RHIC PAC approved a proposal to run a series of six energies to search for the critical point and the onset of deconfinement.
- These energies were run during the 2010 and 2011 running periods.

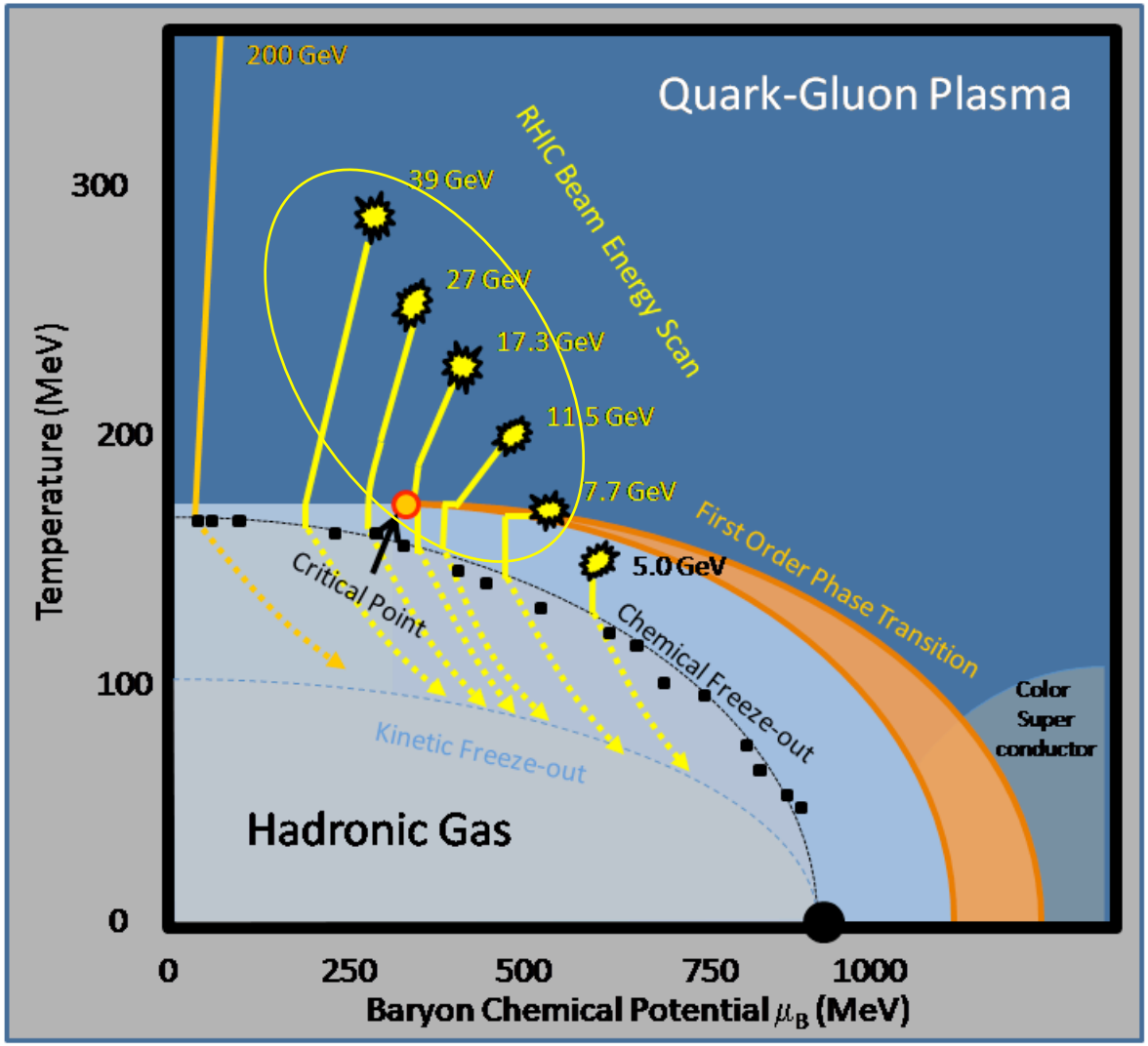

A landmark of the QCD phase diagram

Where are We on the Phase Diagram

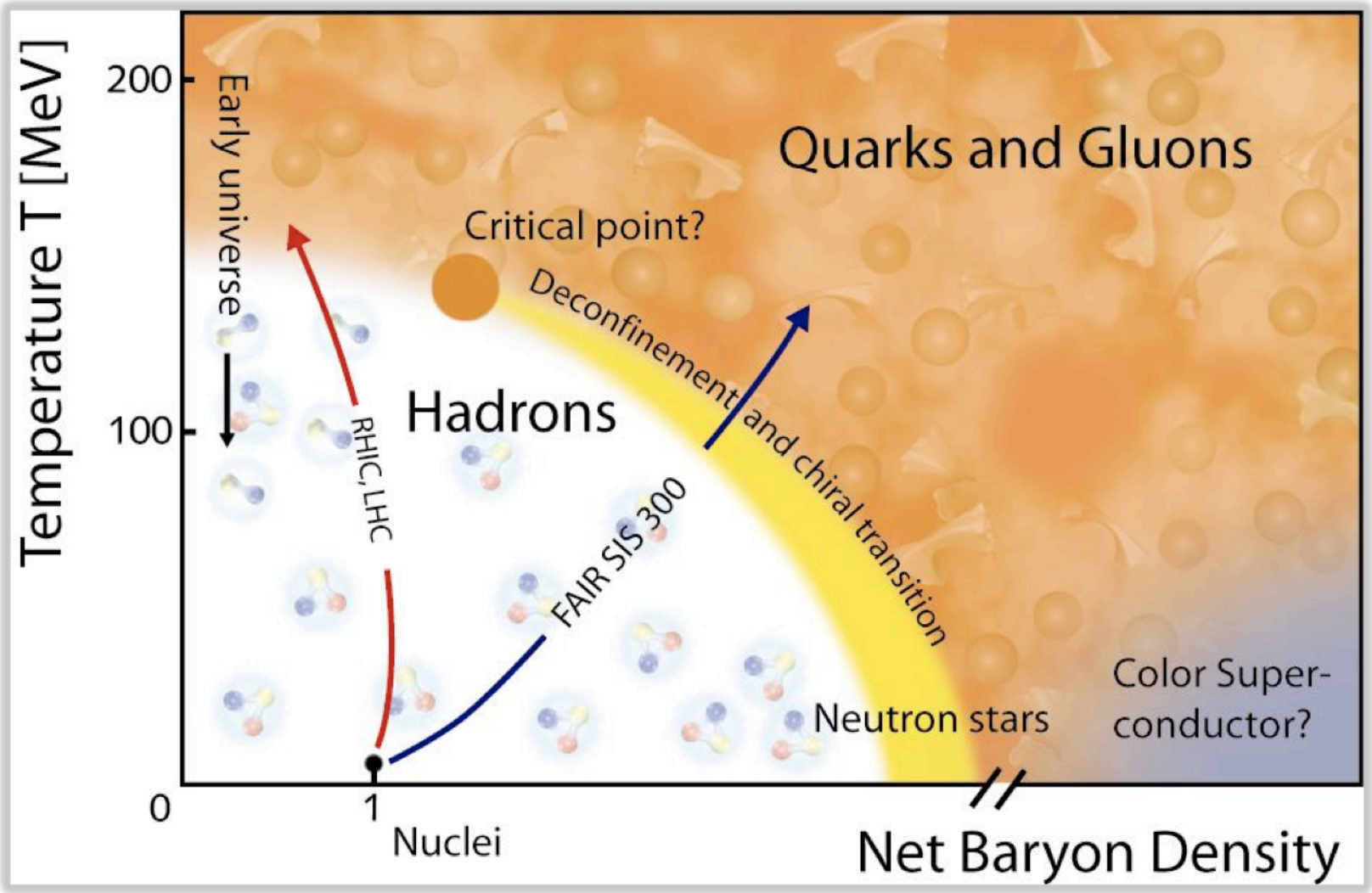

Where are We on the Phase Diagram

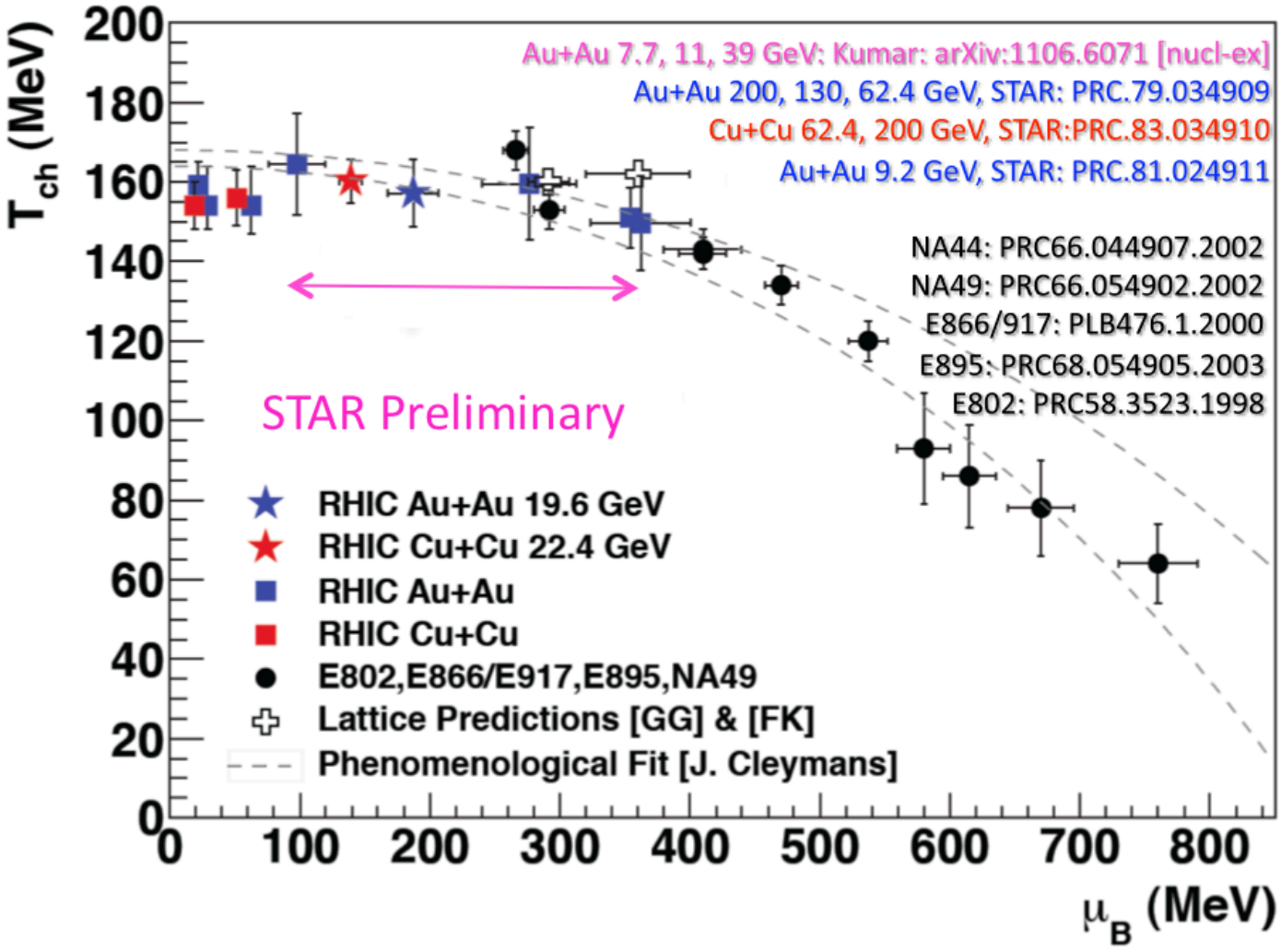

Where are We on the Phase Diagram: BES Result

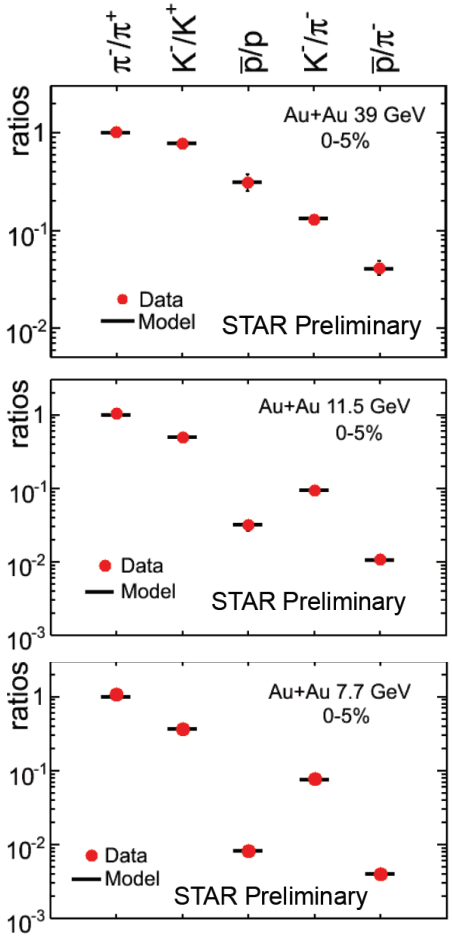

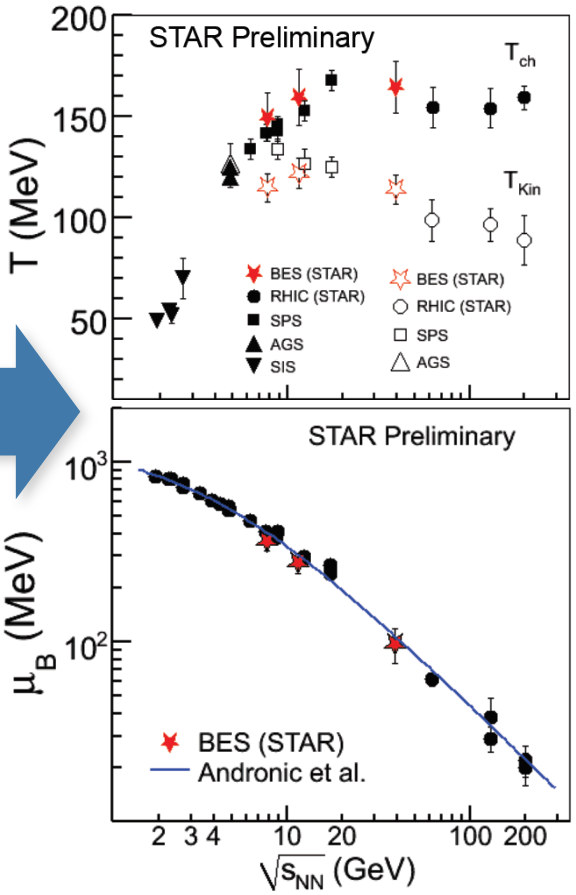

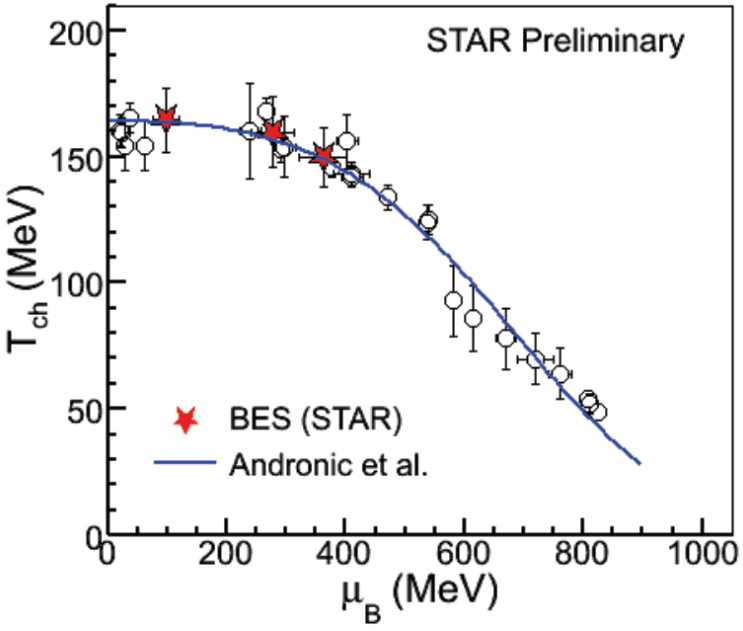

Using the particle ratios from the π, K, and p and a thermal model, we can determine our location on the phase diagram

Directed Flow

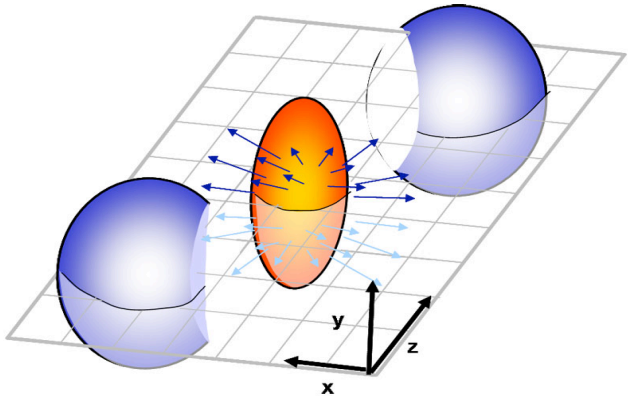

$$\frac{dN}{d\varphi} \propto \left(1 + 2\sum_{n=1}^{+\infty} v_n \cos\left[n(\varphi - \psi_n)\right]\right)$$

Directed flow is quantified by the first harmonic: $v_1 = \langle \cos(\varphi - \psi_1) \rangle$

- Directed flow is due to the sideward motion of the particles within the reaction plane.
- Generated already during the nuclear passage time ($2R/\gamma \approx 3 - 0.1$ fm/c @7.7 – 200 GeV)

⇒ It probes the onset of bulk collective dynamics during thermalization (preequilibrium)

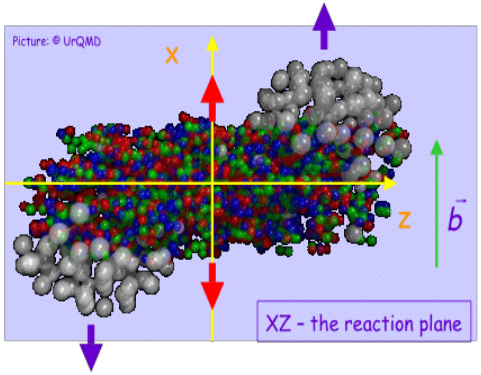

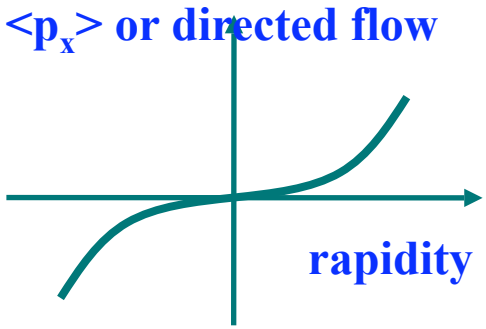

$v_1(y)$ is sensitive to baryon transport, space - momentum correlations and QGP formation

Charged Hadrons v_1: Beam Energy Dependence

Data at 62.4&200GeV from STAR, PRL 101 252301 (2008)

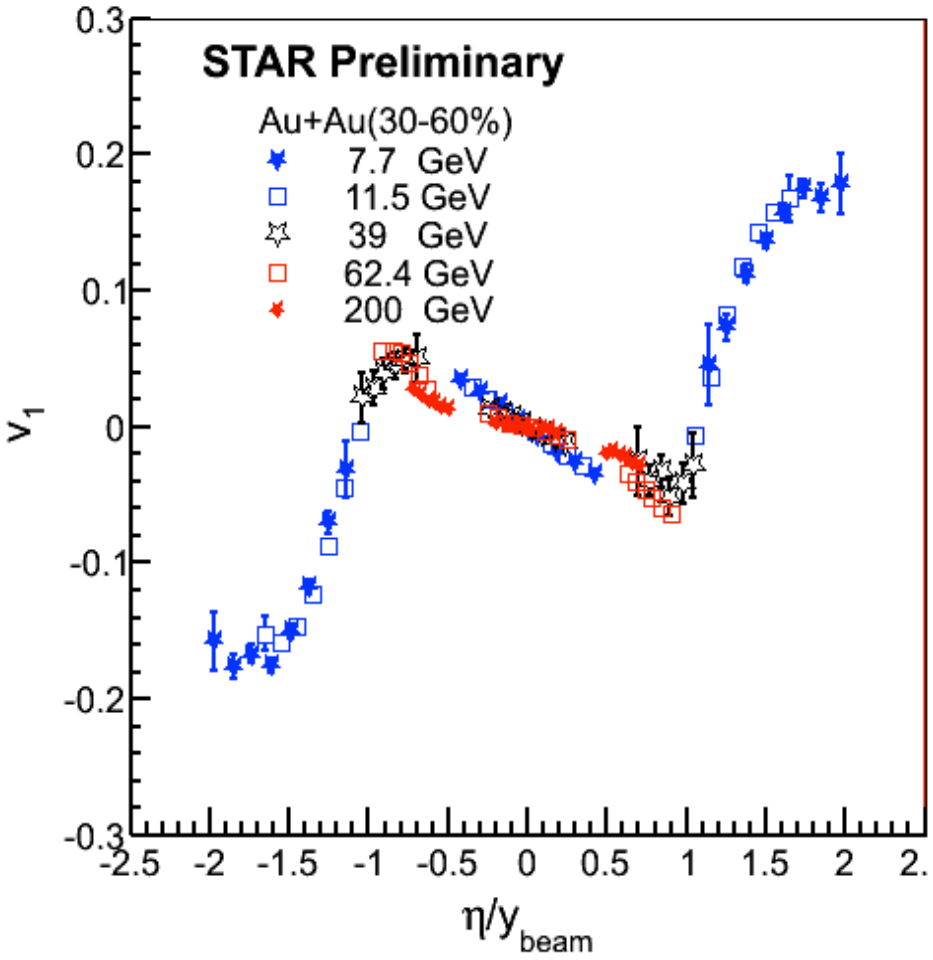

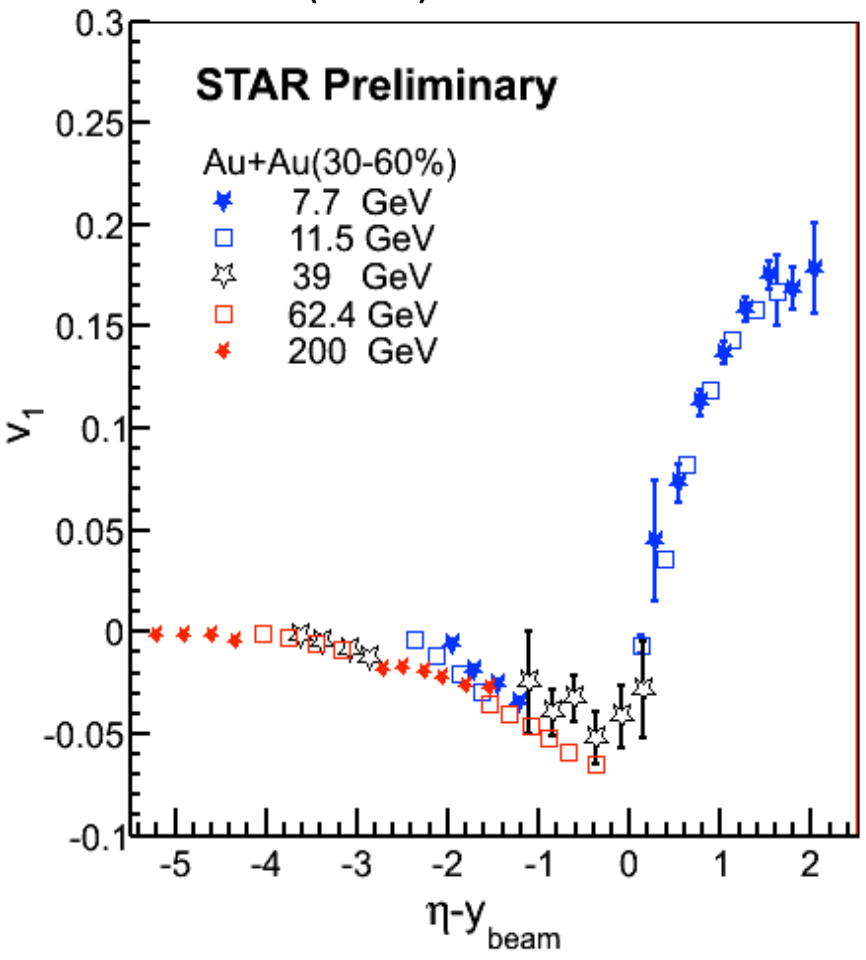

Scaling behavior in v_1 vs. η/y_{beam} and v_1 vs. $\eta'=\eta-y_{beam}$

Directed Flow of Protons: BES Results

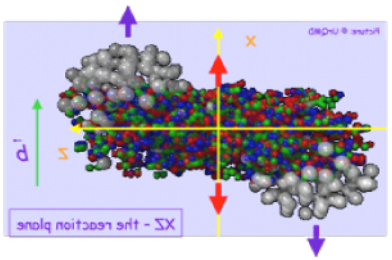

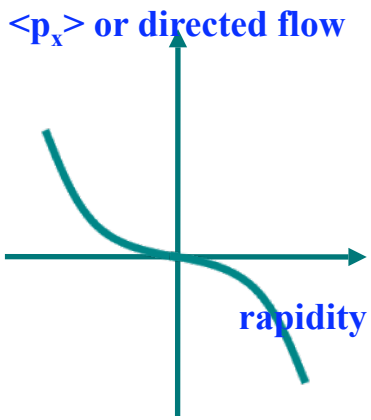

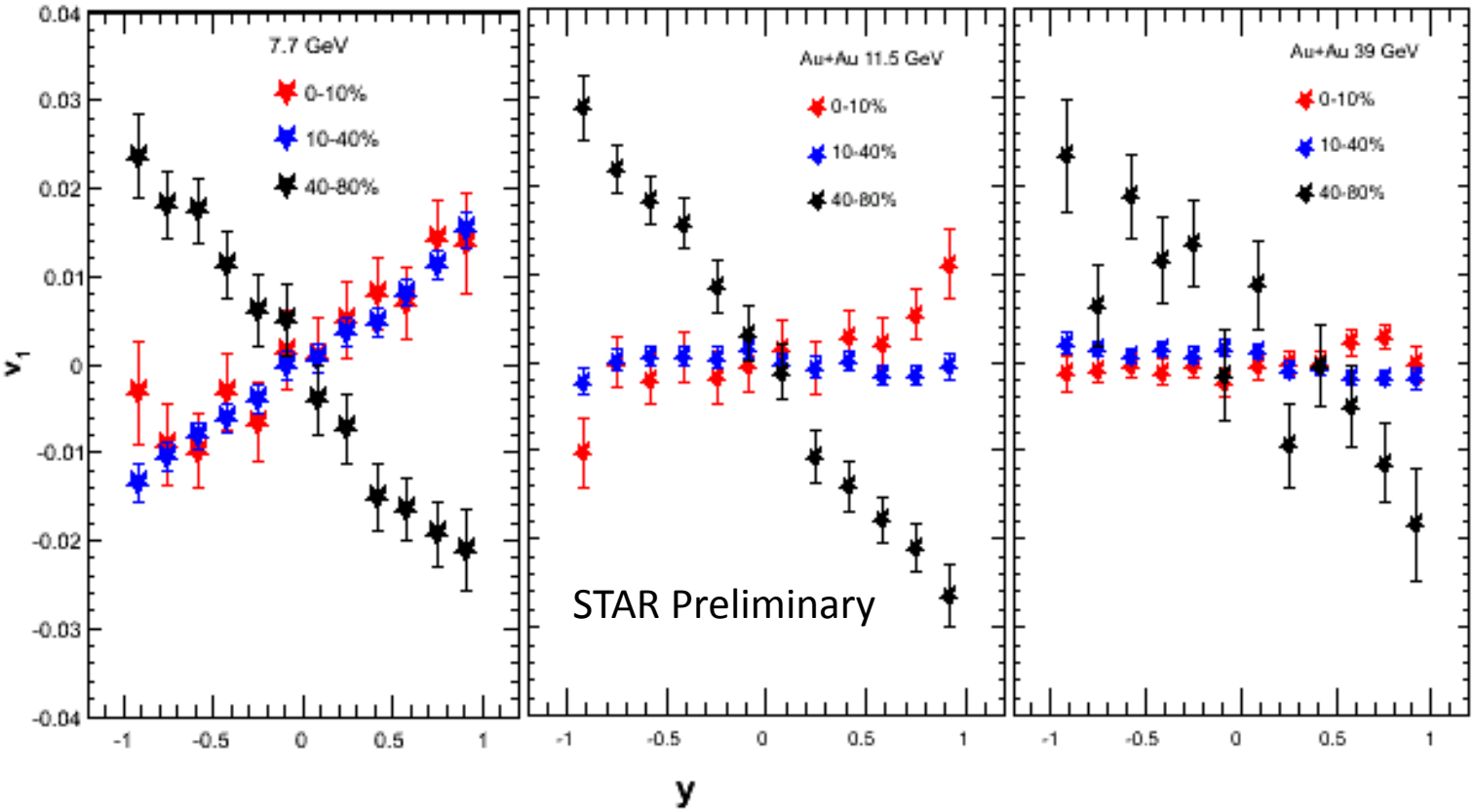

Proton v_1 slope is positive in mid-central collision at 7.7 GeV. At 11.5 GeV, it is almost flat and at 39 GeV and at higher RHIC energies, the proton slope is negative (but small) for mid-central collisions.

The change in proton slope may be due to the contribution from the transported protons coming to midrapidity at the lower beam energies

Elliptic Flow and Collectivity

Initial spatial anisotropy

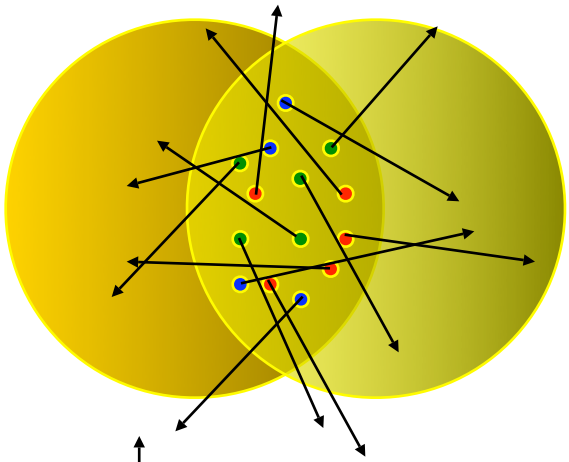

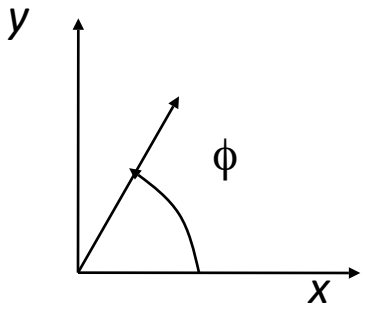

Pressure gradient (EOS)

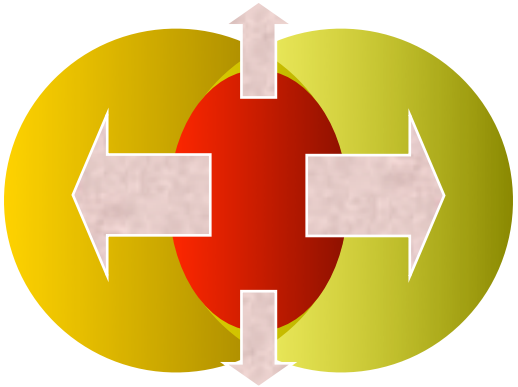

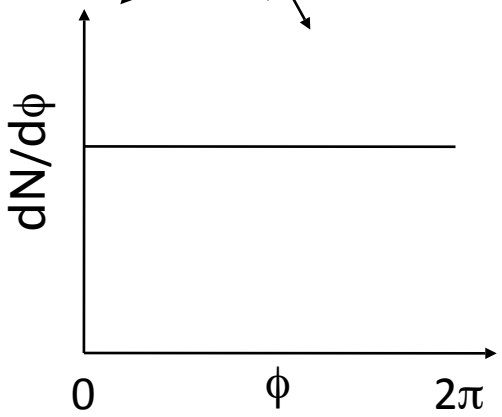

INPUT

Spatial Anisotropy

Interaction among produced particles

OUTPUT

Momentum Anisotropy

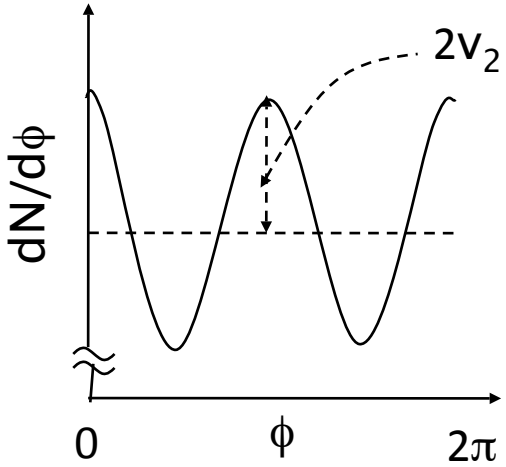

$$\lambda=(\sigma\rho)^{-1}$$

$$\varepsilon_x = \left\langle \frac{y^2 - x^2}{y^2 + x^2} \right\rangle$$

$$v_2 = \langle \cos 2\varphi \rangle = \left\langle \frac{p_x^2 - p_y^2}{p_x^2 + p_y^2} \right\rangle$$

Adapted from B. Mohanty

Free streaming v_2=0

Energy Dependence of Elliptic Flow

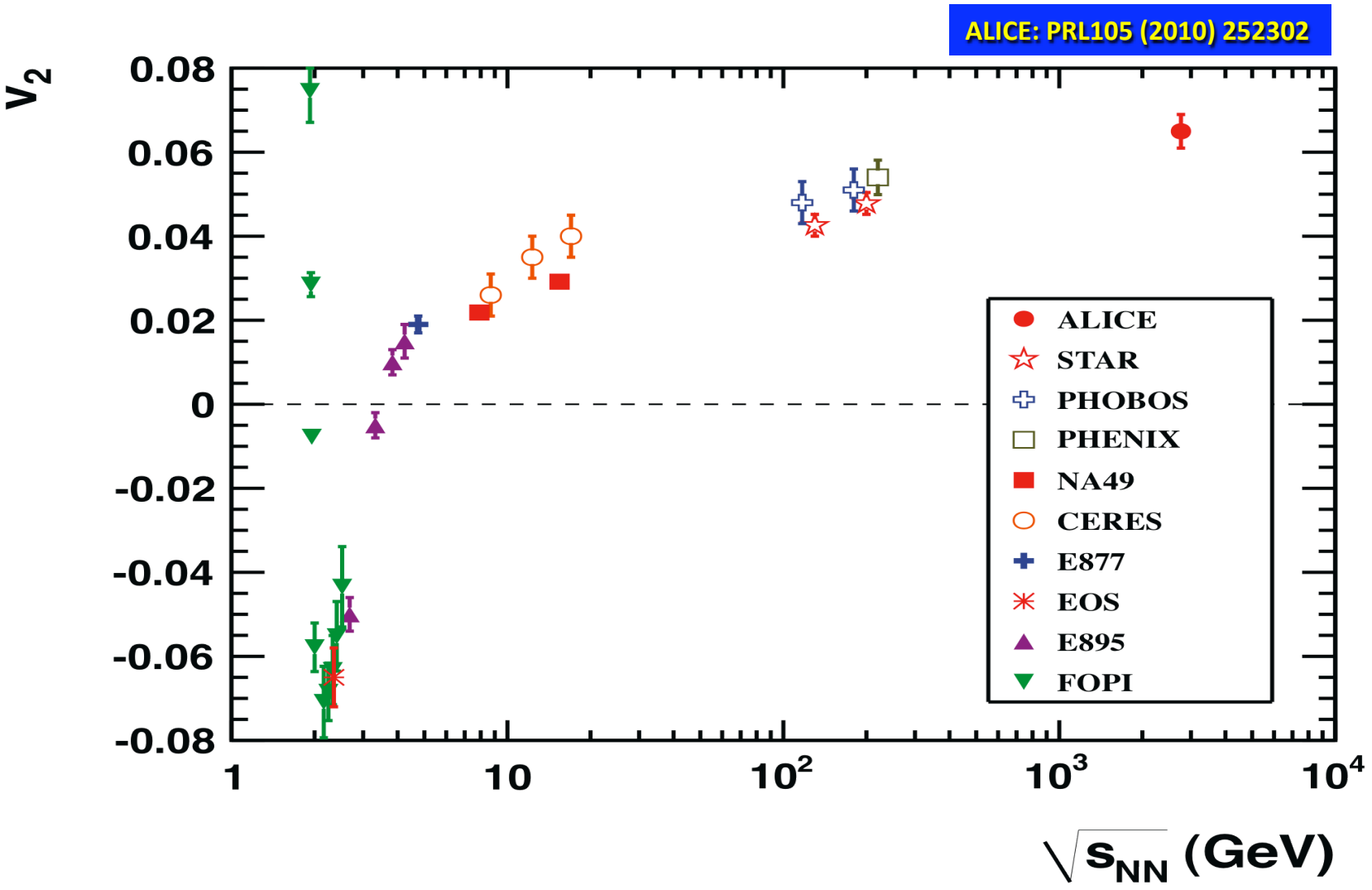

$v_2(p_T)$: Au+Au at 39/62.4/200 GeV

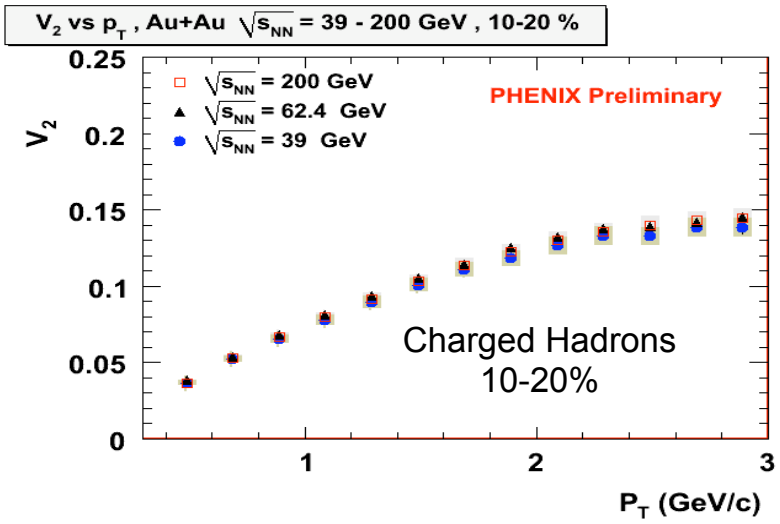

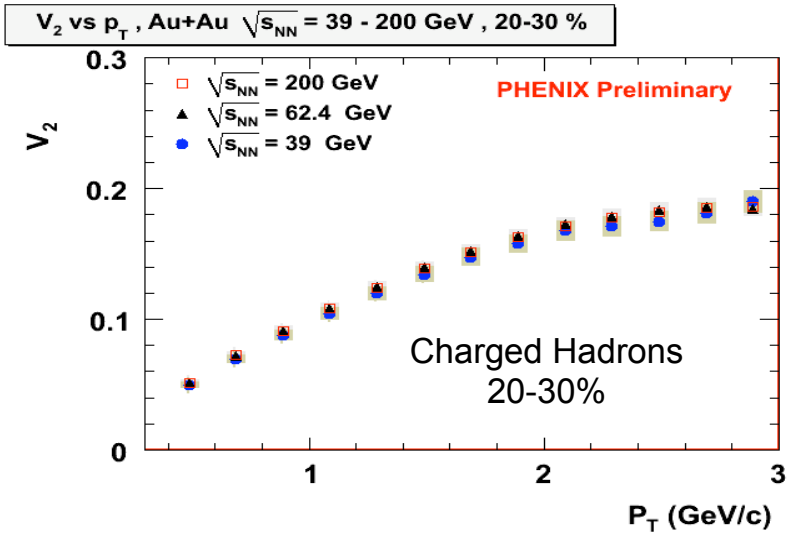

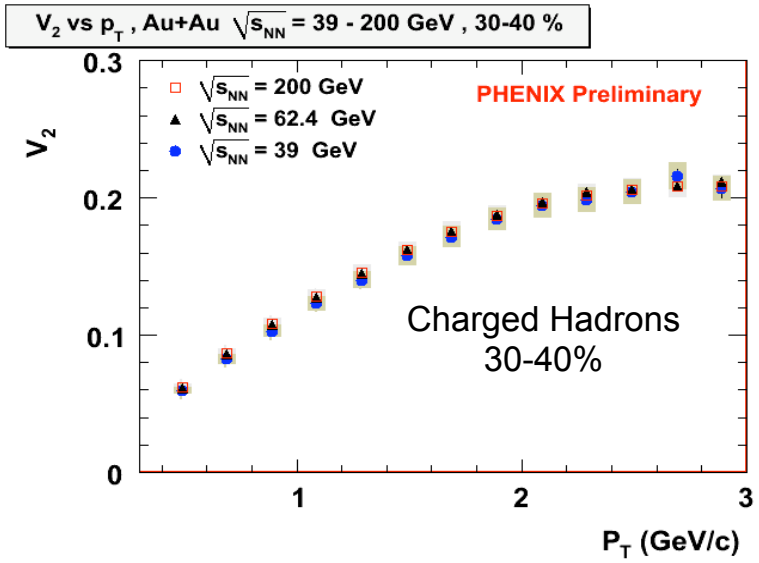

$v_2(p_T)$: Au+Au at 39/62.4/200 GeV

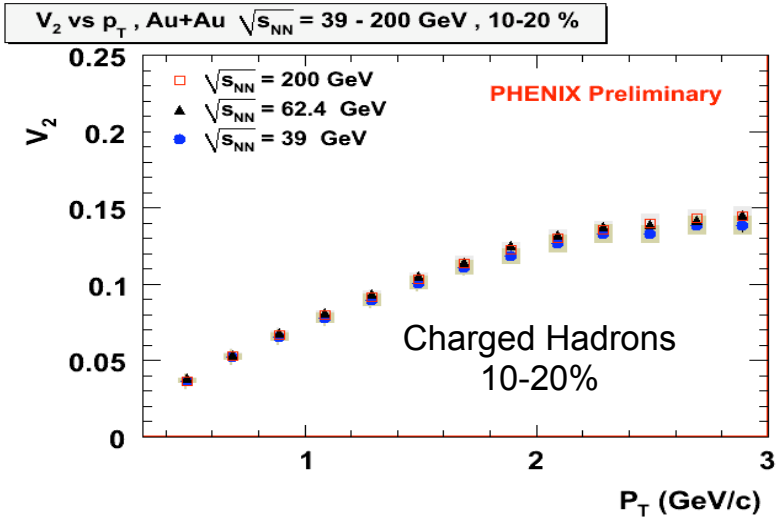

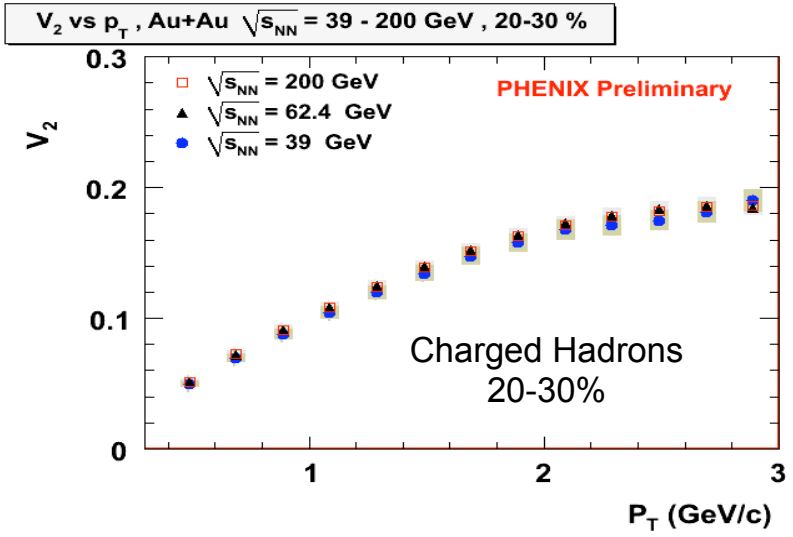

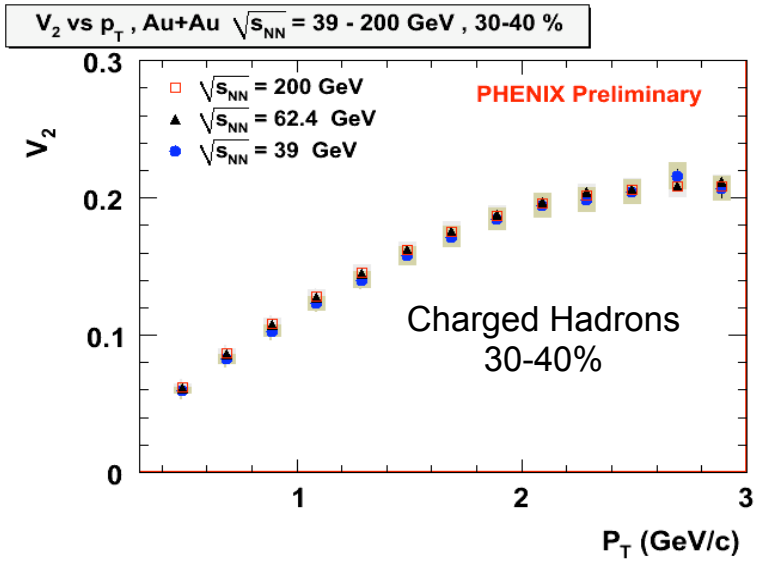

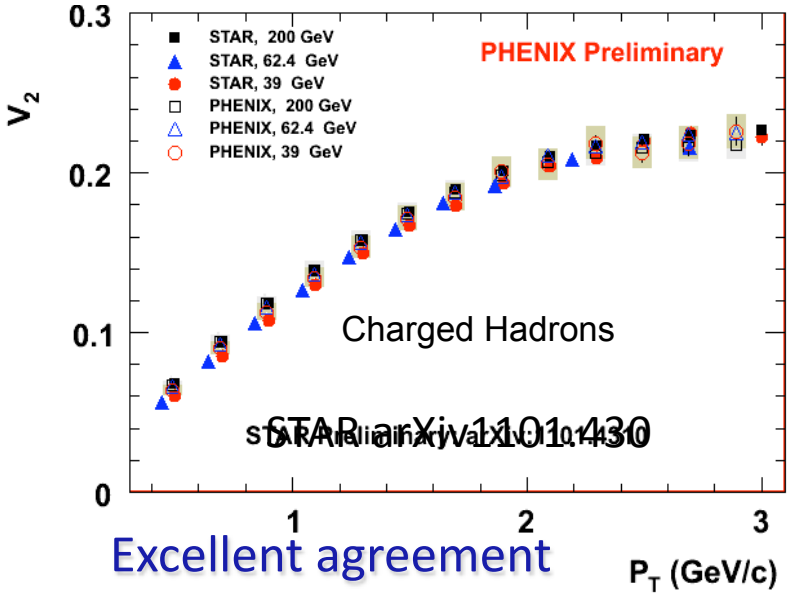

Similar hydro-properties from 39 to 200 GeV

Excellent agreement between experiments for $\sqrt{s_{NN}}$=39-200 GeV

$v_2(p_T)$ at RHIC and LHC

STAR: PRC 77 (2008) 054901; PRC 75 (2007) 054906

ALICE: PRL105 (2010) 252302

STAR: Nucl.Phys. A862-863 (2011) 125

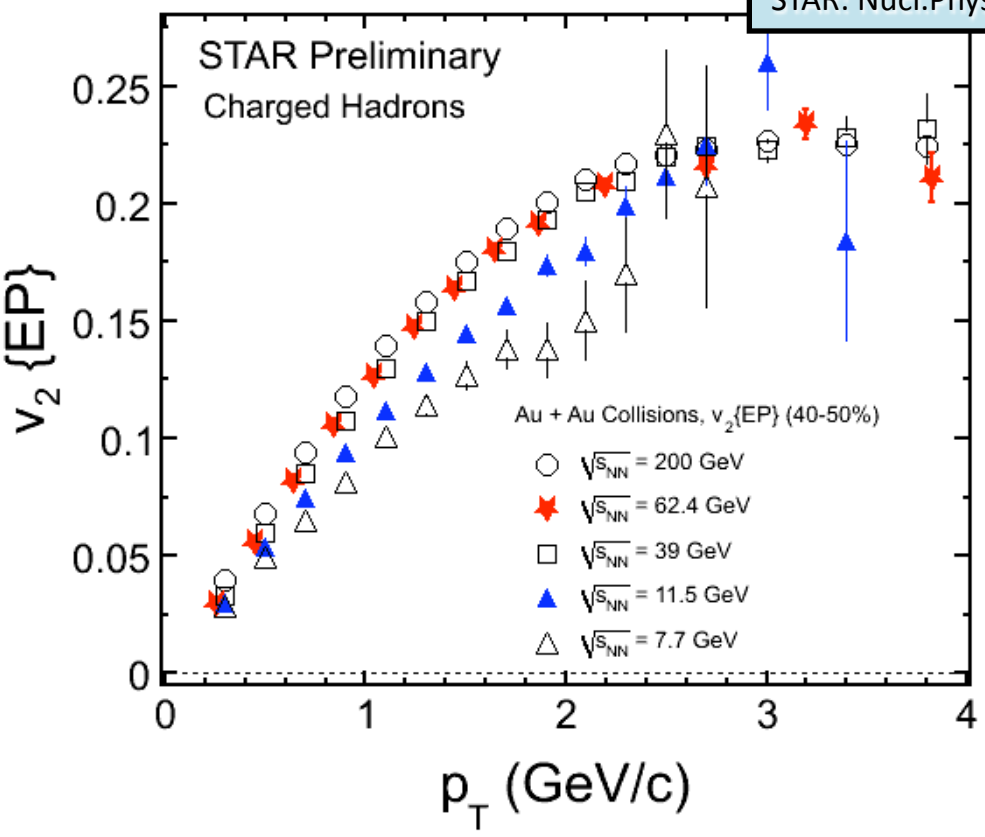

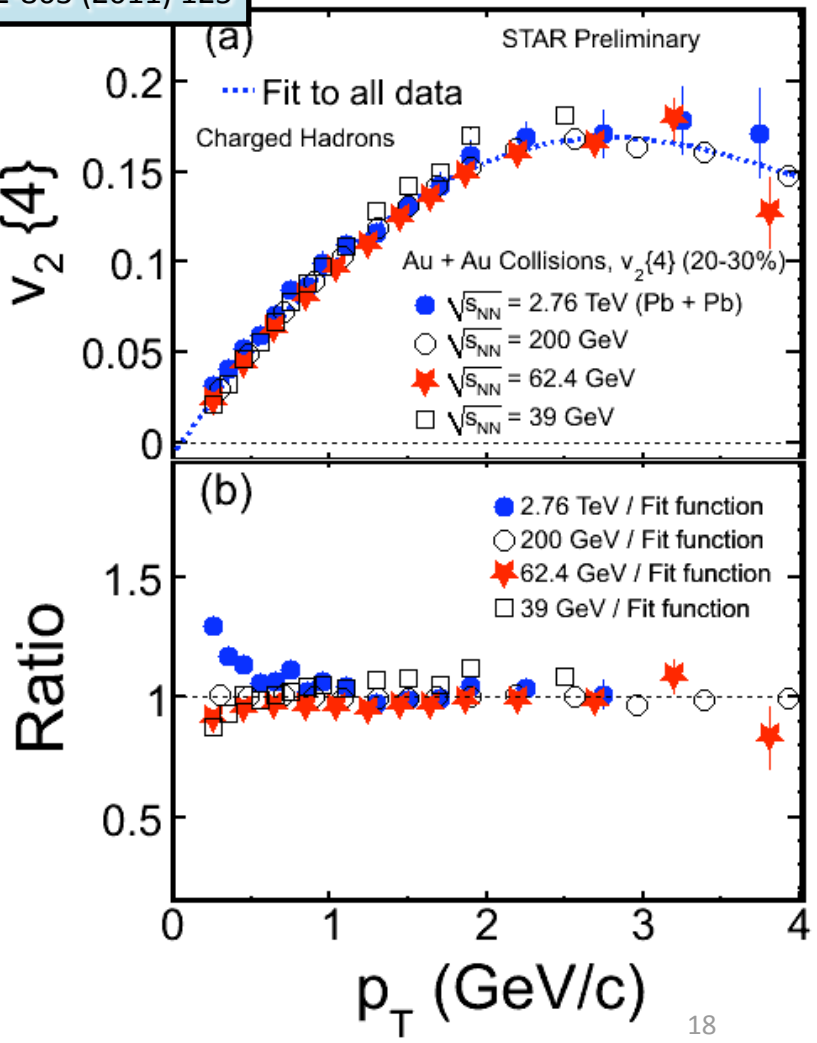

$v_2(p_T)$ at RHIC and LHC

STAR: PRC 77 (2008) 054901; PRC 75 (2007) 054906

ALICE: PRL105 (2010) 252302

STAR: Nucl.Phys. A862-863 (2011) 125

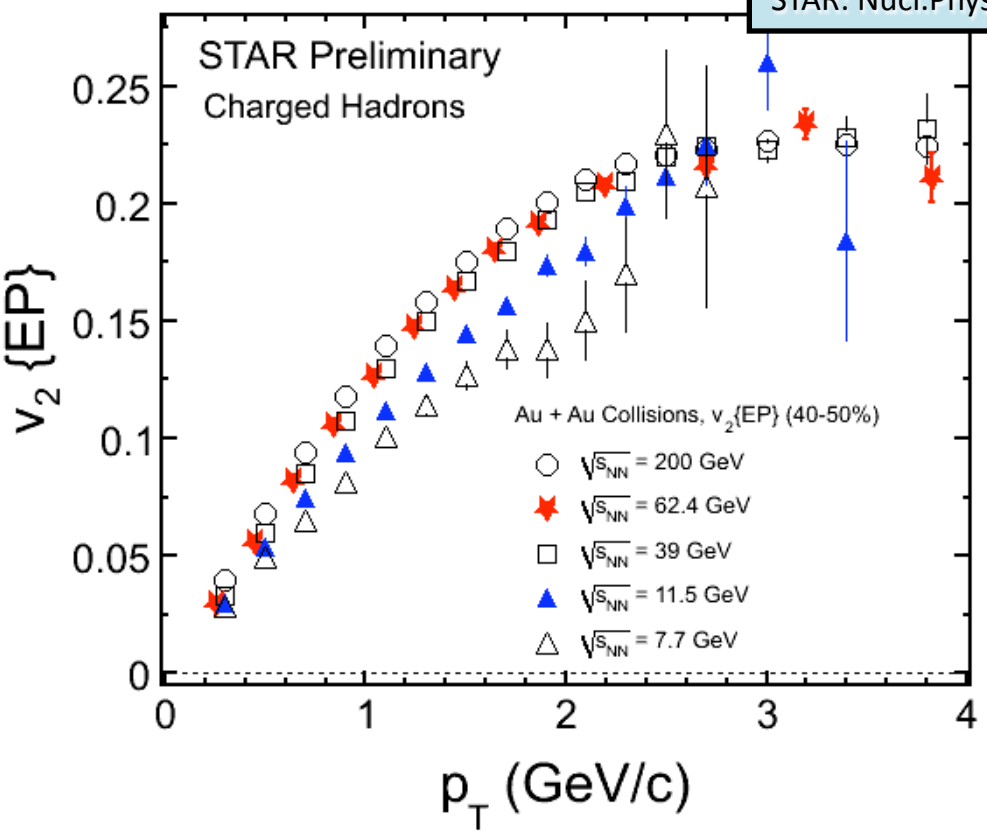

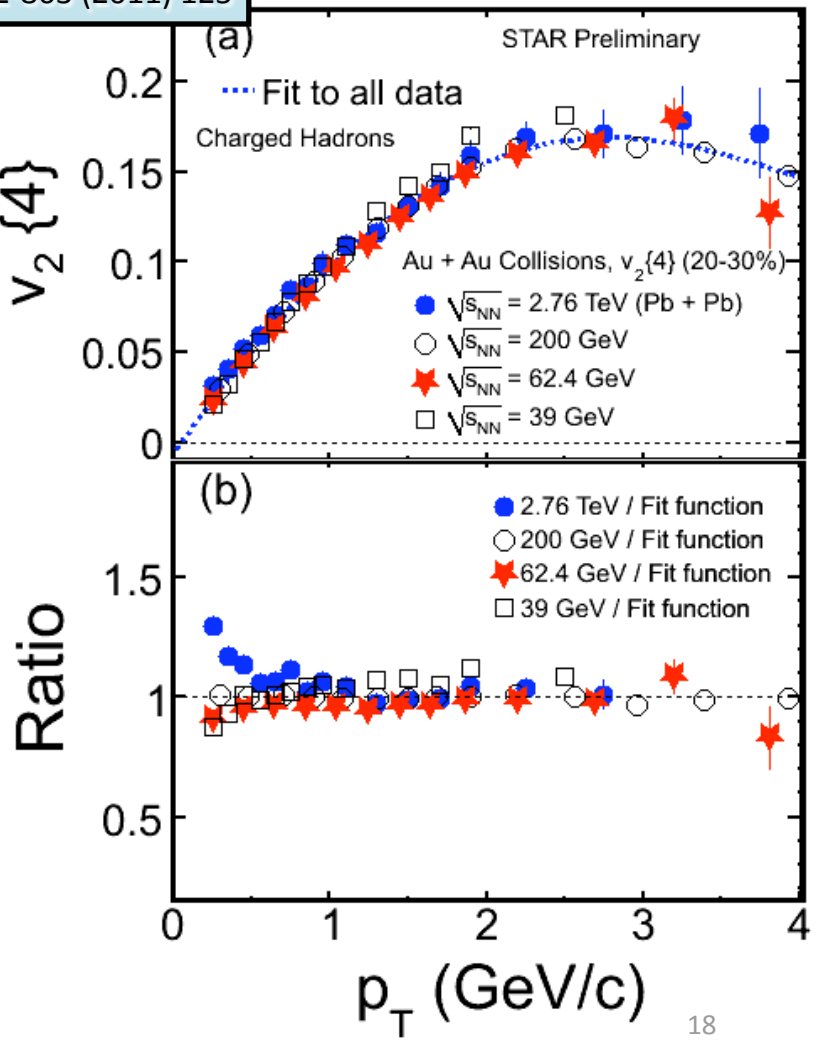

✓ v_2 (7.7 GeV) < v_2 (11.5 GeV) < v_2 (39 GeV)

$v_2(p_T)$ at RHIC and LHC

STAR: PRC 77 (2008) 054901; PRC 75 (2007) 054906

ALICE: PRL105 (2010) 252302

STAR: Nucl.Phys. A862-863 (2011) 125

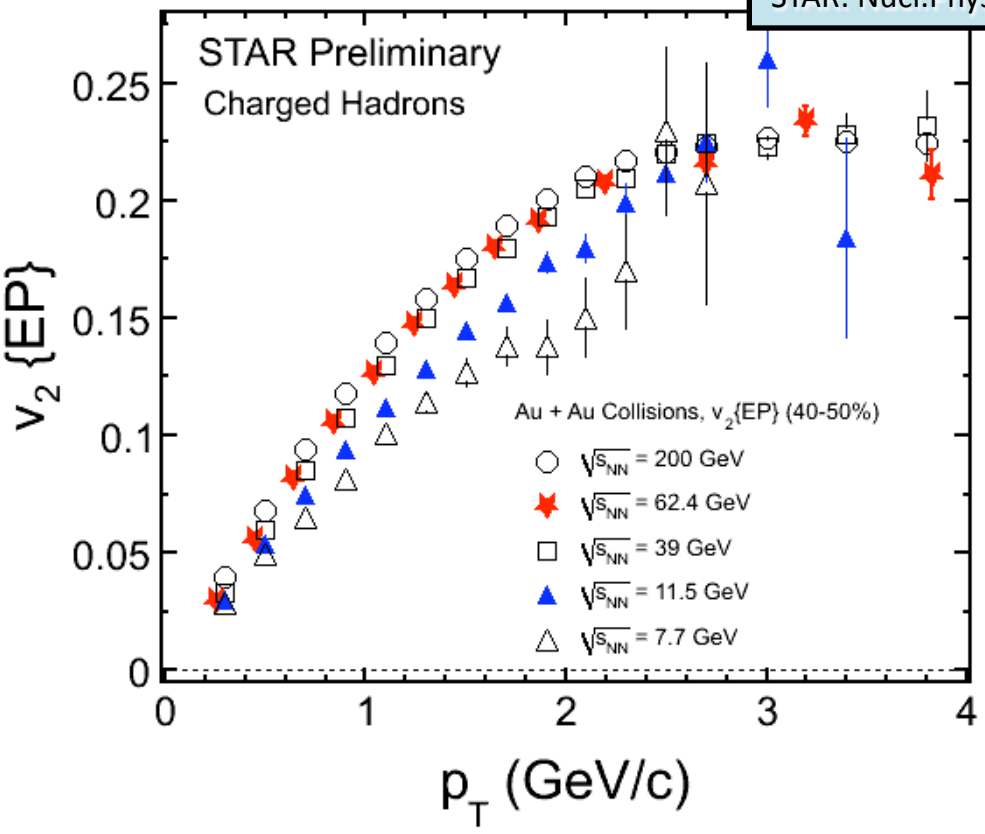

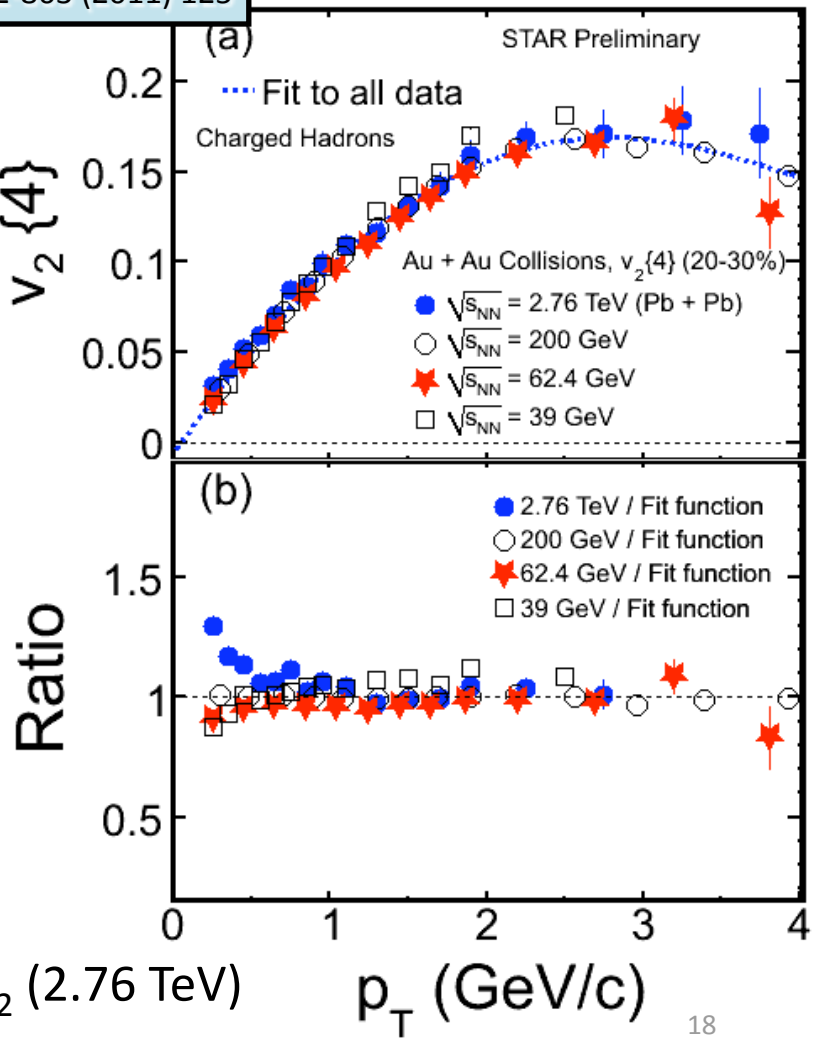

✓ v_2 (7.7 GeV) < v_2 (11.5 GeV) < v_2 (39 GeV)

★ v_2 (39 GeV) ≈ v_2 (62.4 GeV) ≈ v_2 (200 GeV) ≈ v_2 (2.76 TeV)

Comparable $v_2(p_T)$ from 39GeV to 2.76TeV

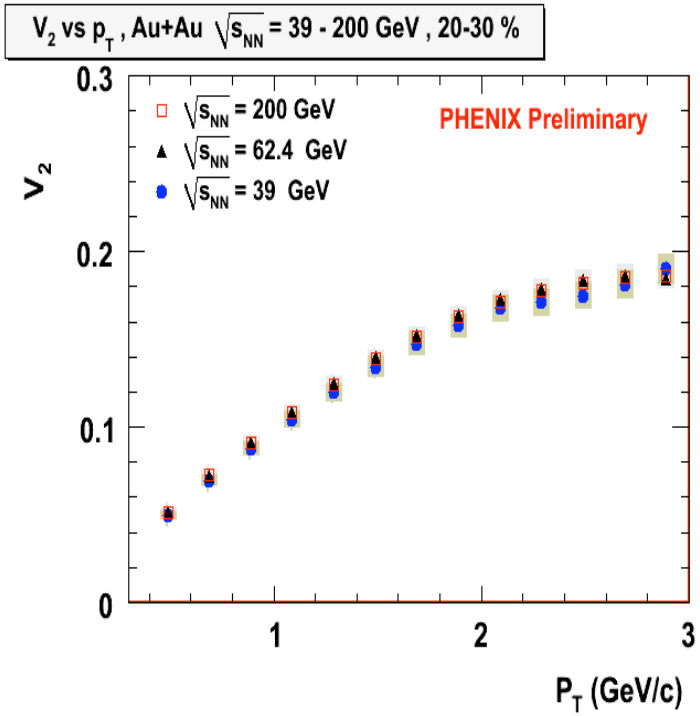

ALICE Experiment, PRL105,252302 (2010)

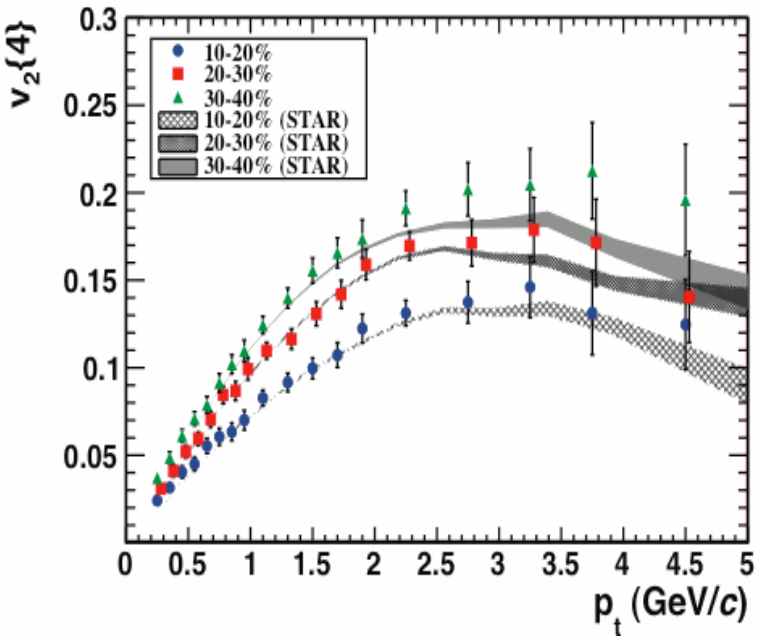

Comparable $v_2(p_T)$ from 39GeV to 2.76TeV

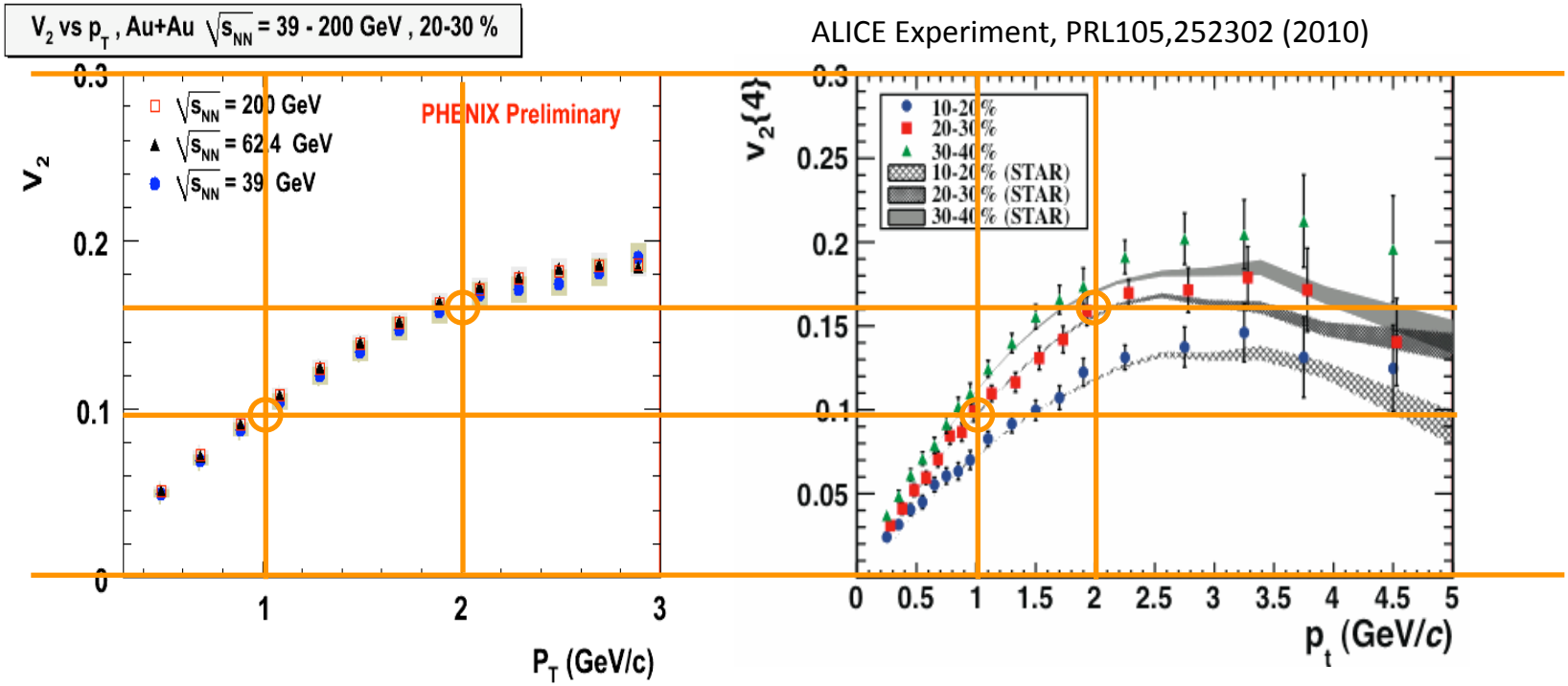

Comparable $v_2(p_T)$ from 39GeV to 2.76TeV

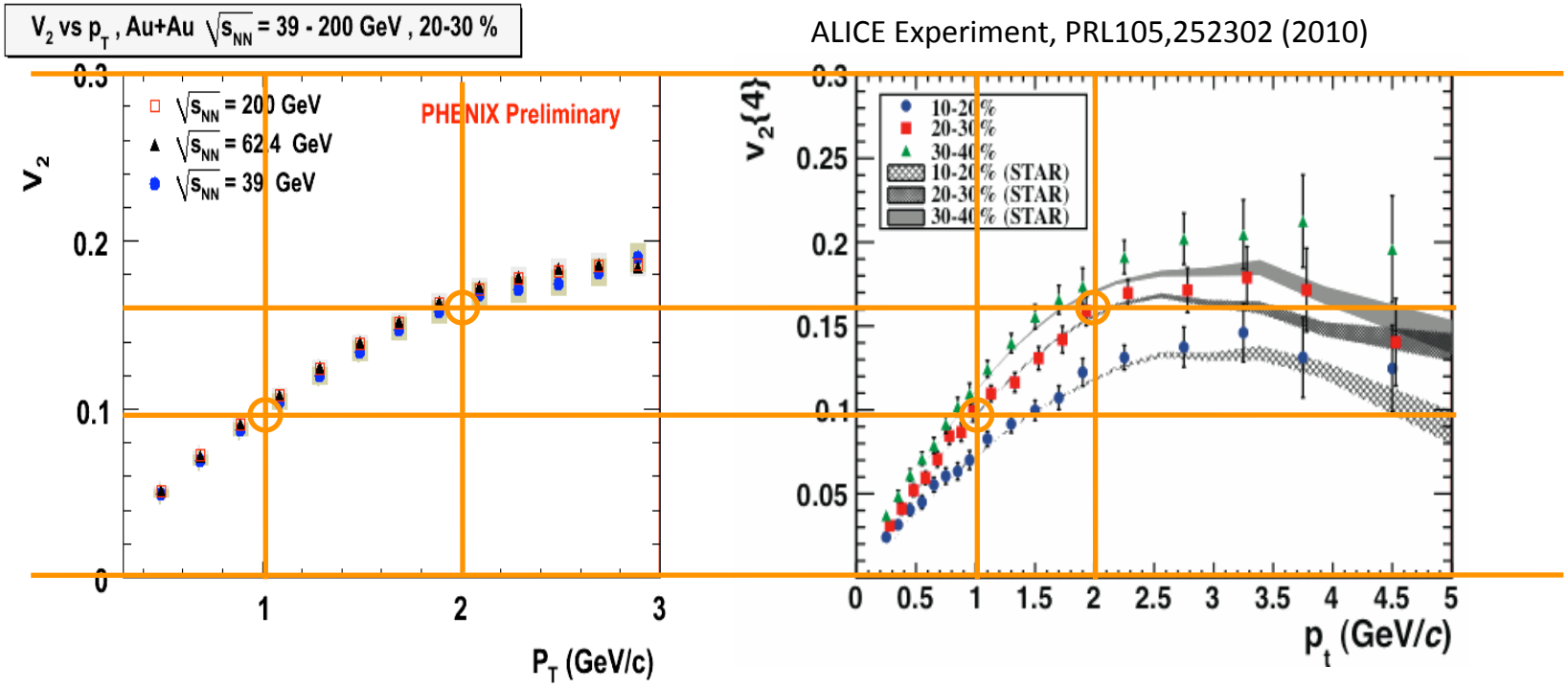

⇒ Energy dependence of v_2 is driven by the change in $\langle p_T \rangle$

✓ The same flow properties from $\sqrt{s_{NN}}$=39 GeV to 2.76 TeV

Flow: What are the Relevant d.o.f.

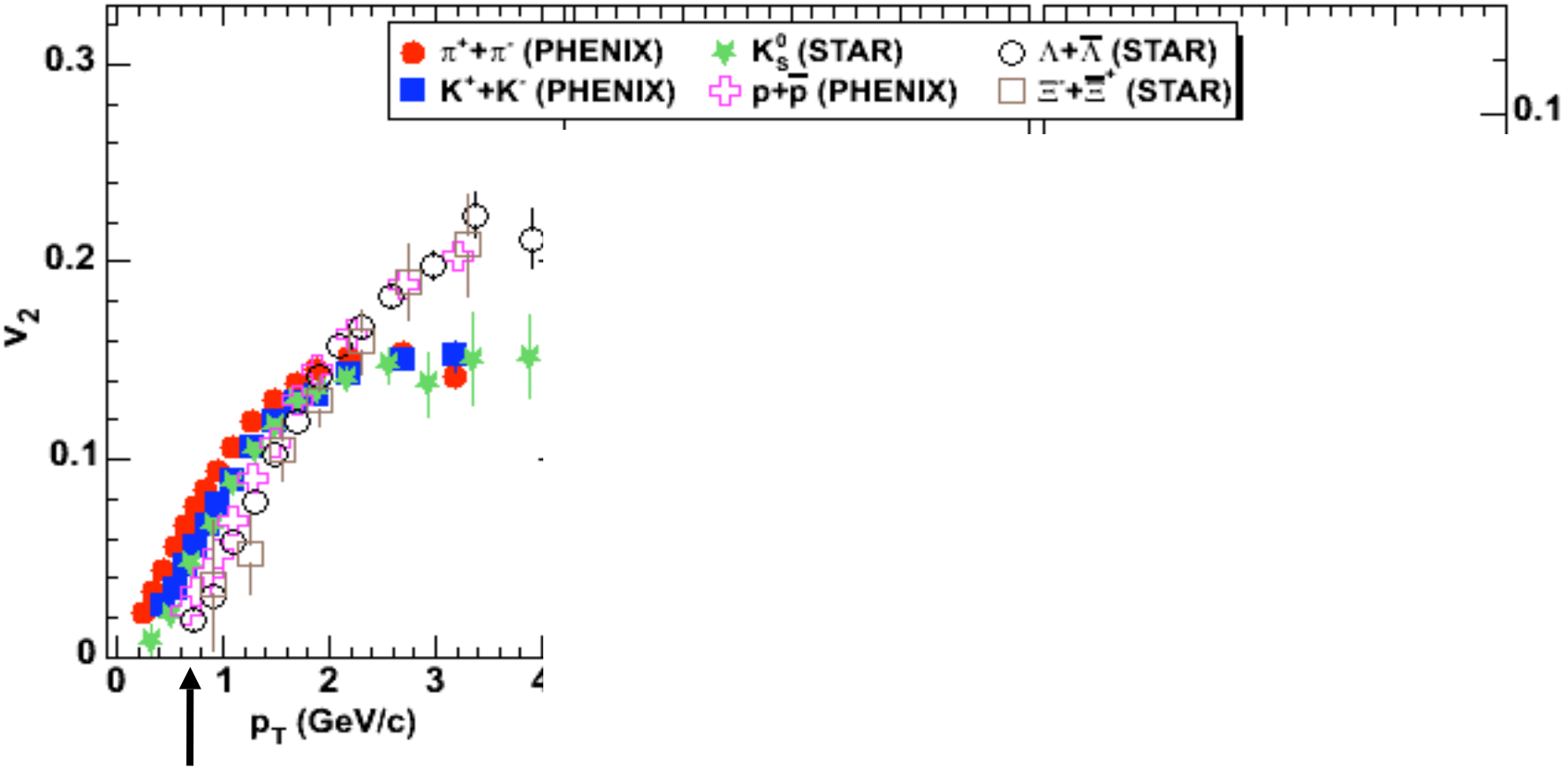

particle mass dependence

STAR: PRL **95**, 122301 (2005)

PHENIX: PRL **98**, 162301 (2007)

Flow: What are the Relevant d.o.f.

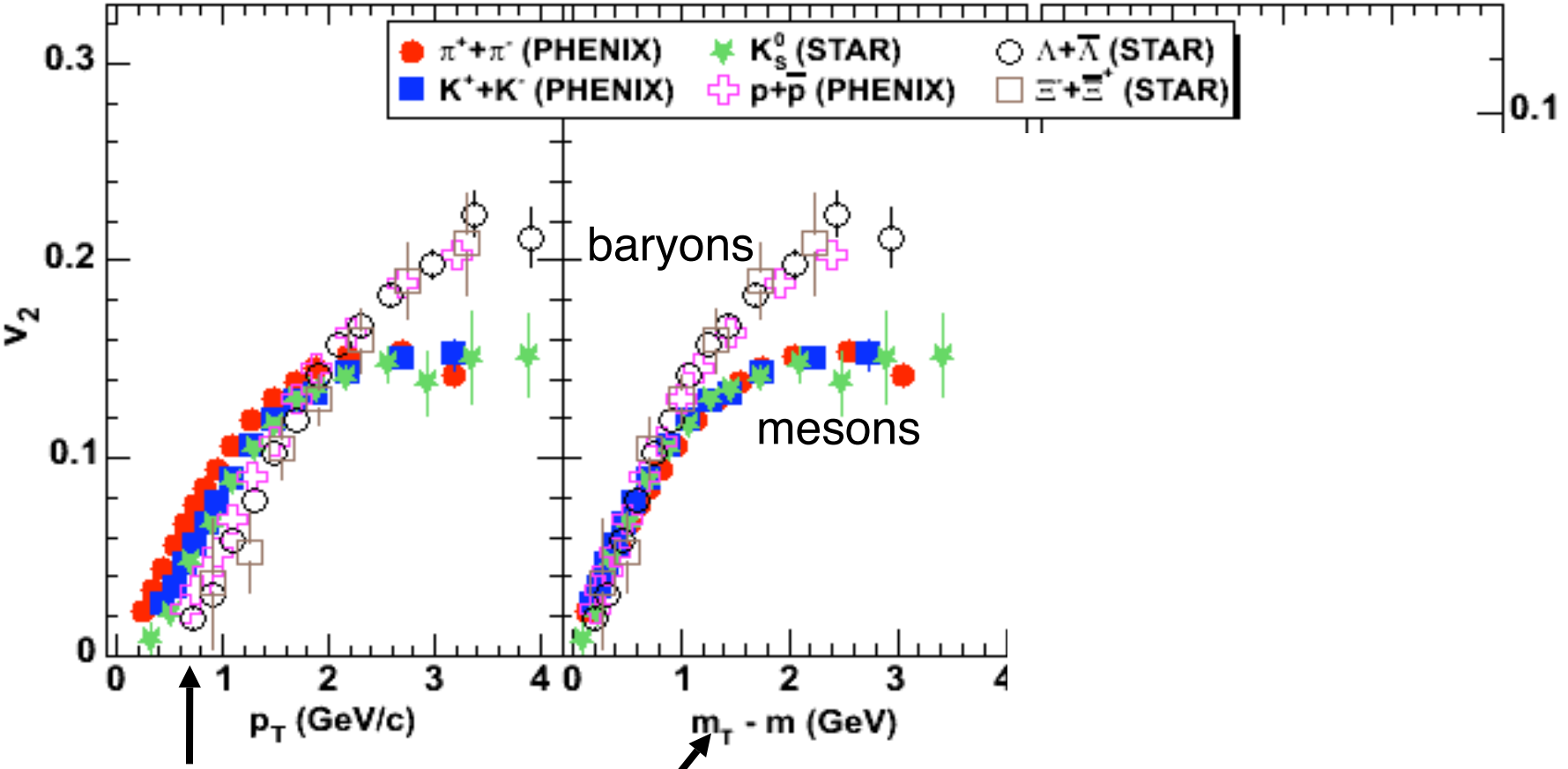

particle mass dependence

plotted vs. trans. kinetic energy

STAR: PRL **95**, 122301 (2005)

PHENIX: PRL **98**, 162301 (2007)

Flow: What are the Relevant d.o.f.

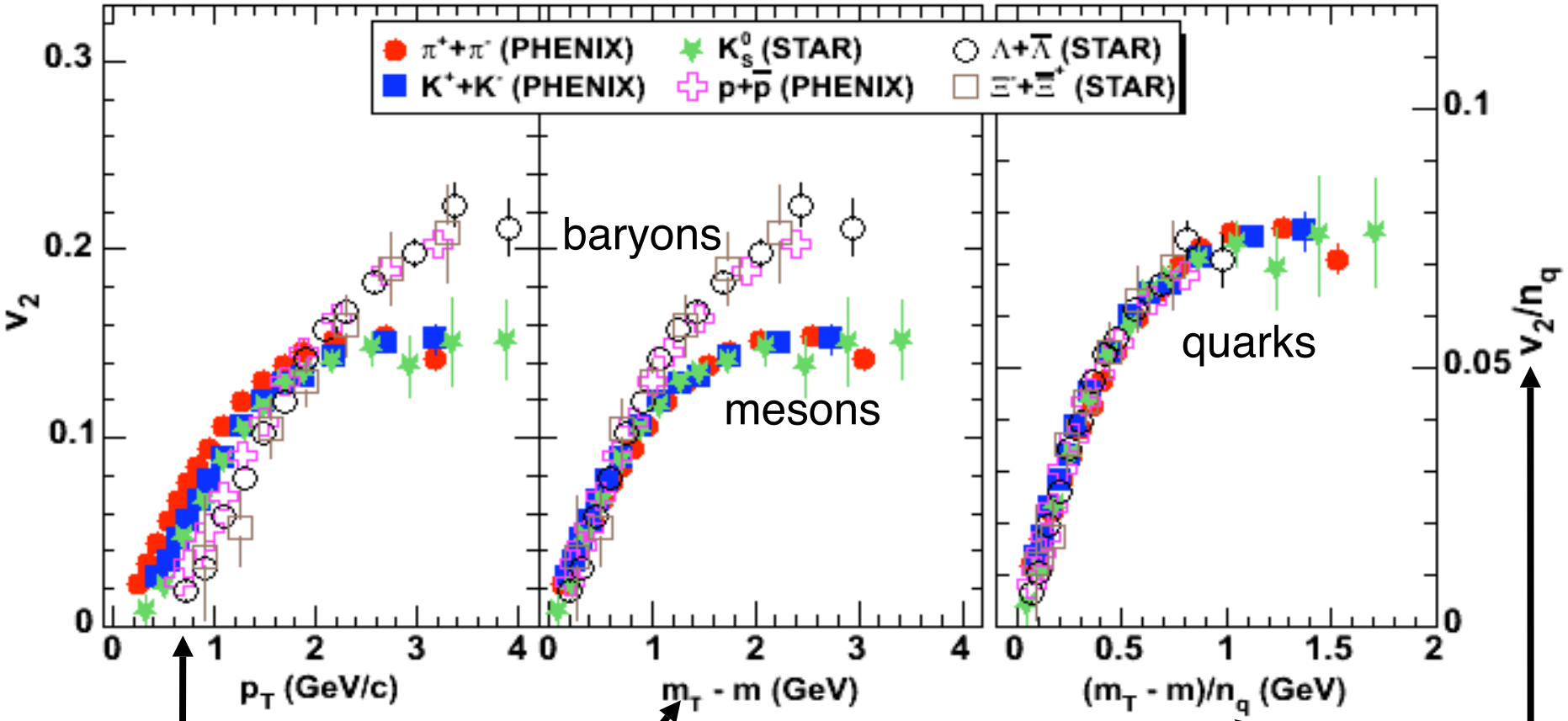

particle mass dependence

plotted vs. trans. kinetic energy

both axes scaled by number of constituent quarks

recombination of constituent quarks
quarks acquire v_2 before hadronization

$n_q = 2$ for mesons

$n_q = 3$ for baryons

STAR: PRL **95**, 122301 (2005)

PHENIX: PRL **98**, 162301 (2007)

Fluid of Constituent Quarks

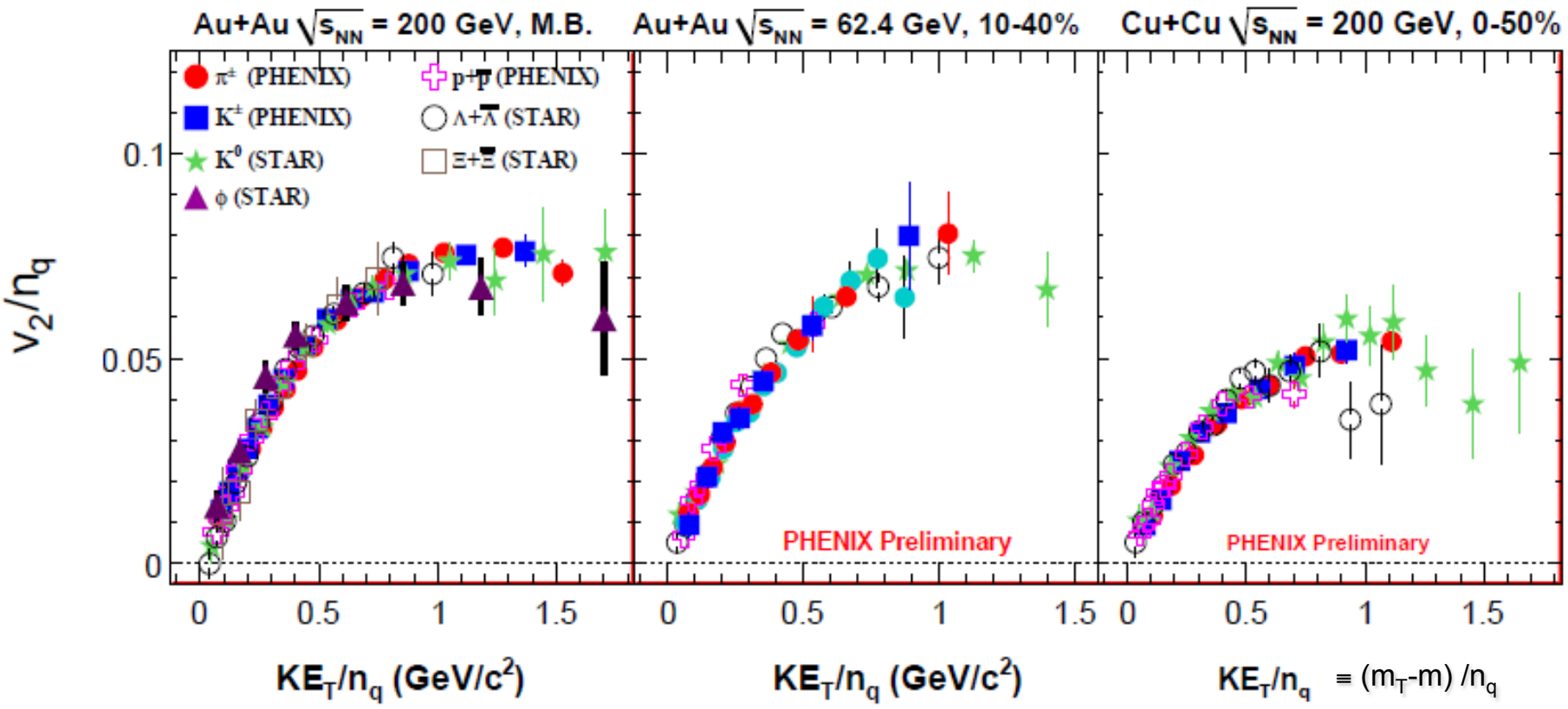

Fluid of Constituent Quarks

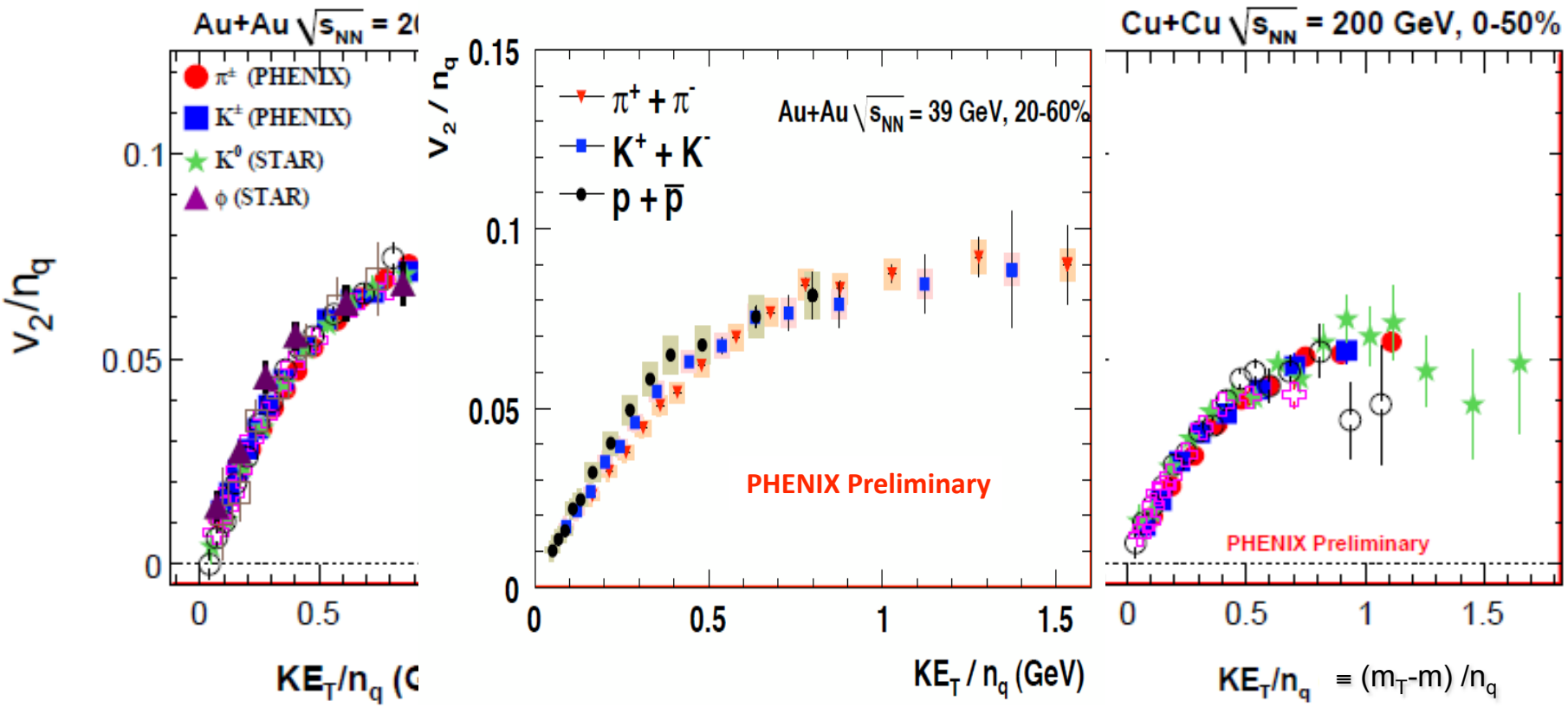

Fluid of Constituent Quarks

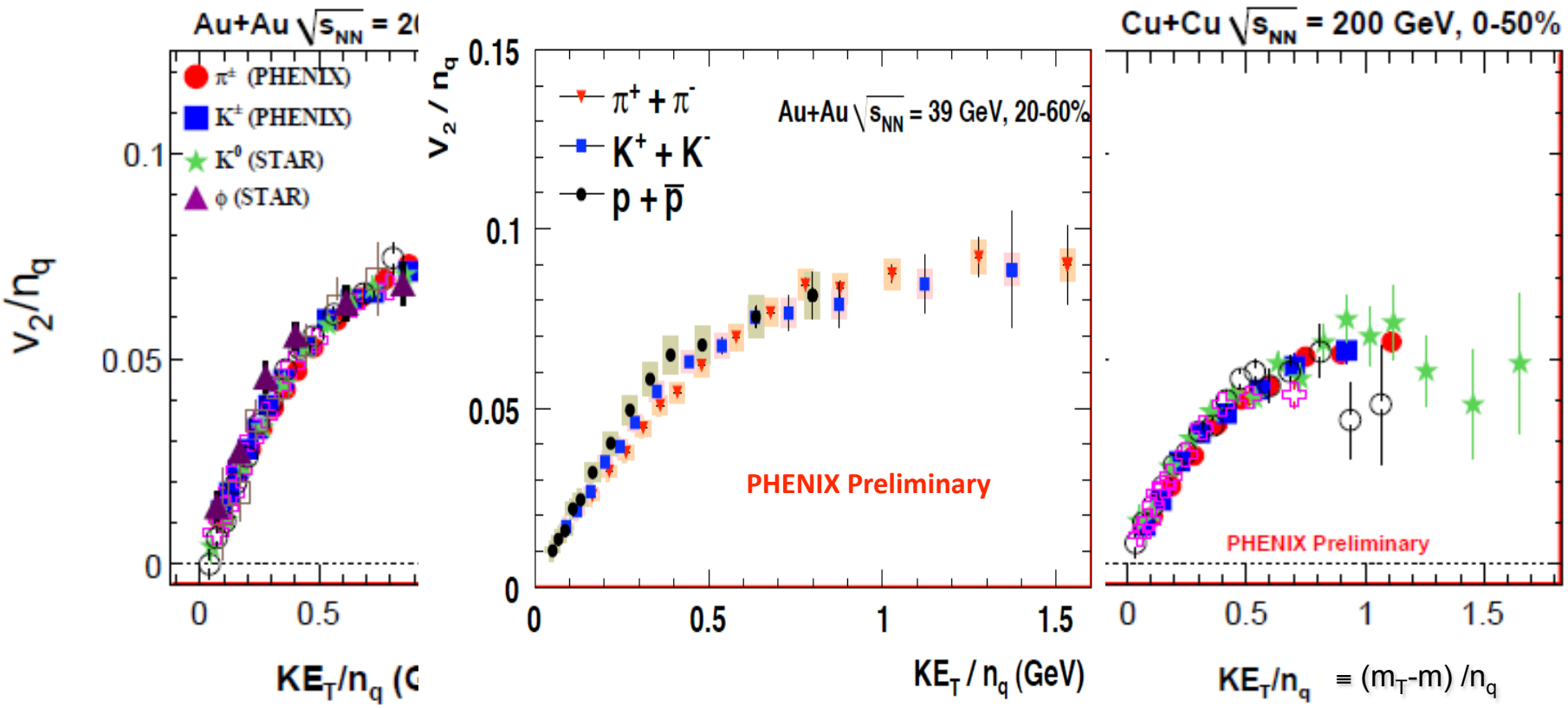

✓ From 39 GeV to 200 GeV the same d.o.f. are relevant for the flow

✓ BES goal: find the energy where the effect starts to turn off

BES Result: n_{cq}-scaling of ϕ meson?

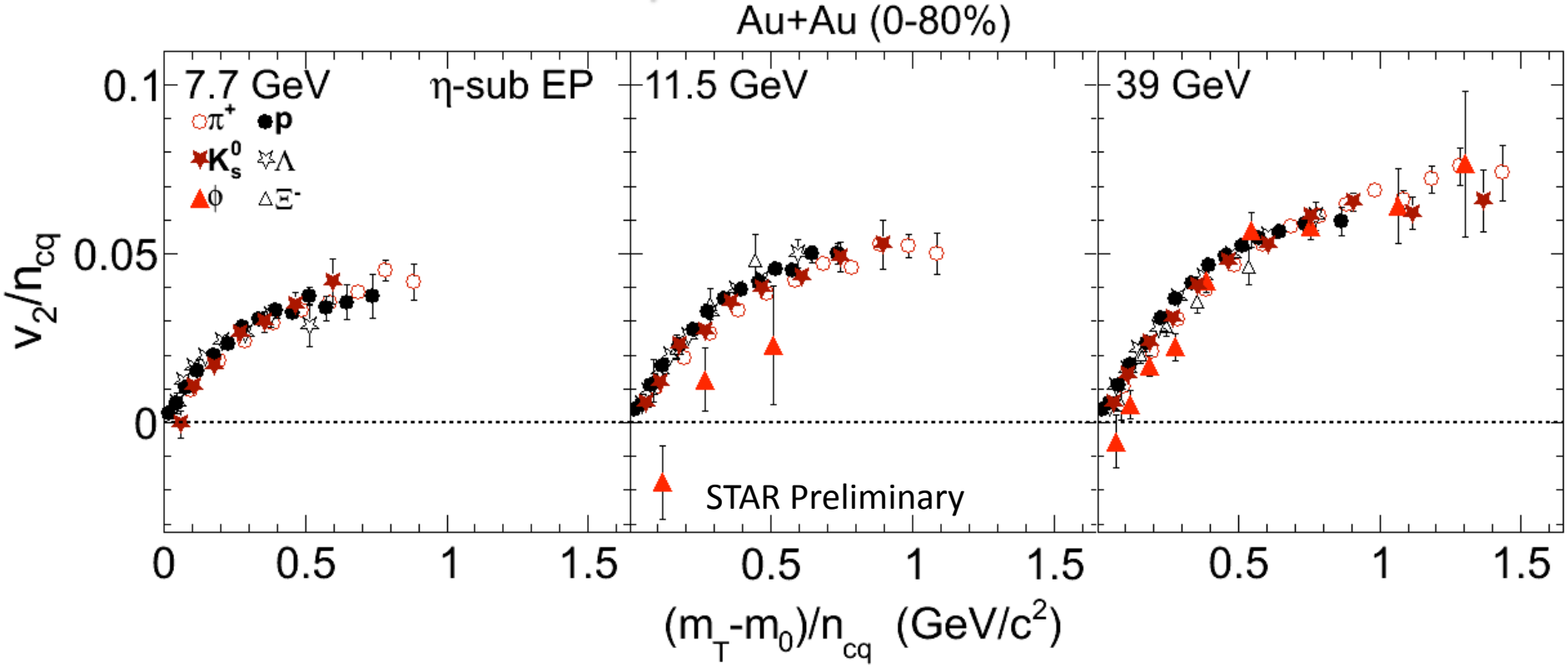

- ✓ Universal trend for most of particles – n_{cq} scaling not broken at low energies
- ➢ ϕ meson v_2 deviates from other particles in Au+Au@11.5 GeV:

  Mean deviation from pion distribution: 0.02±0.008 (→ 2.6 σ)

  Low hadronic cross section of ϕ → less partonic flow seen ?

  Reduction of v_2 for ϕ meson and absence of n_{cq} scaling ➔ during the evolution the system remains in the hadronic phase

[B. Mohanty and N. Xu; J. Phys. G 36

Beyond the v_2: Higher Order Harmonics

For smooth profile odd harmonics cancel out

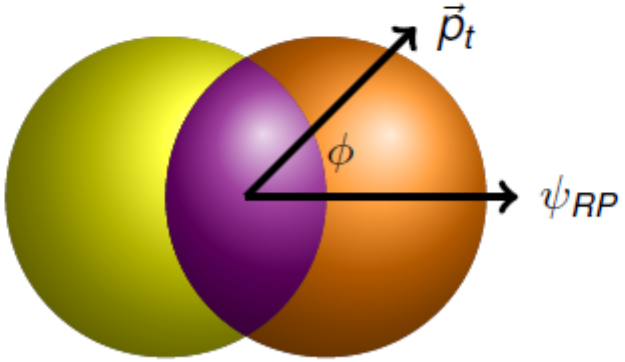

$$\frac{dN}{d\varphi} \propto \left(1 + 2\sum_{n=1}^{+\infty} v_n \cos\left[n(\varphi - \psi_n)\right]\right)$$

Beyond the v_2: Higher Order Harmonics

For smooth profile odd harmonics cancel out

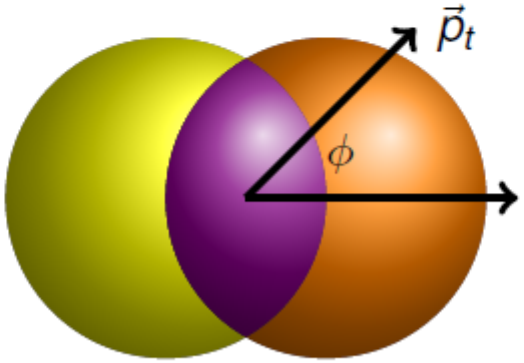

The initial collision geometry is "lumpy"

No particular symmetry

$v_{n+1} \neq 0$ (event-by-event)

For "lumpy" profile odd harmonics persist

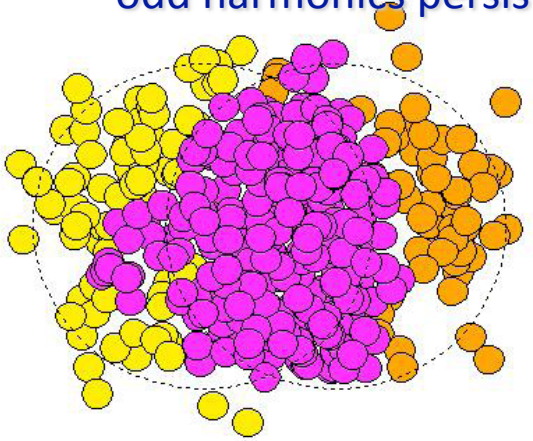

Beyond the v_2: Higher Order Harmonics

For smooth profile odd harmonics cancel out

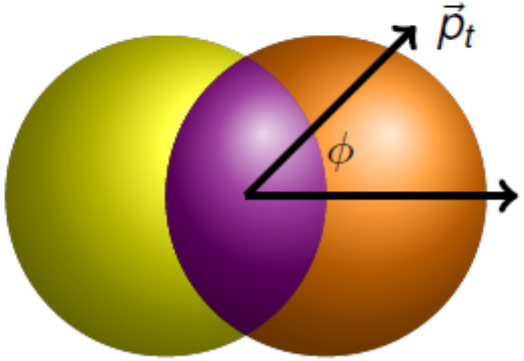

The initial collision geometry is "lumpy"

No particular symmetry

$v_{n+1} \neq 0$ (event-by-event)

For "lumpy" profile odd harmonics persist

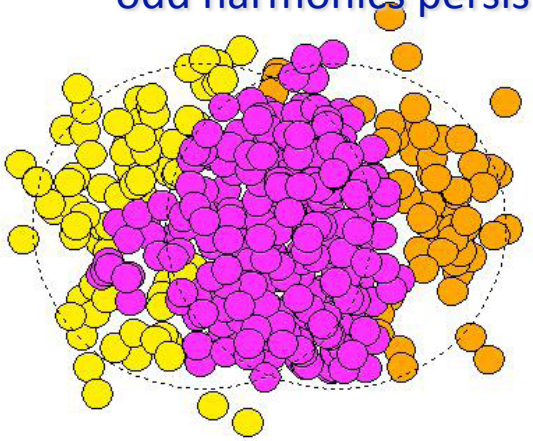

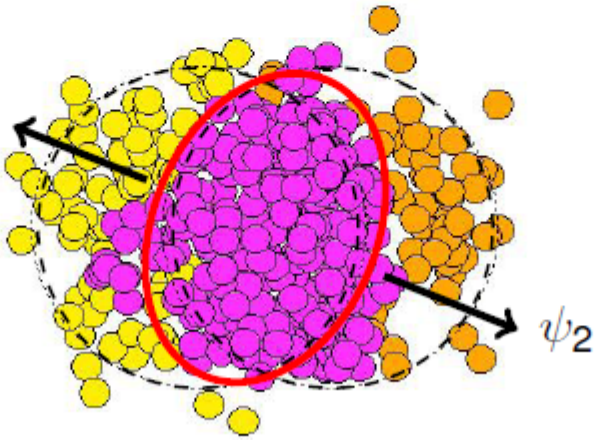

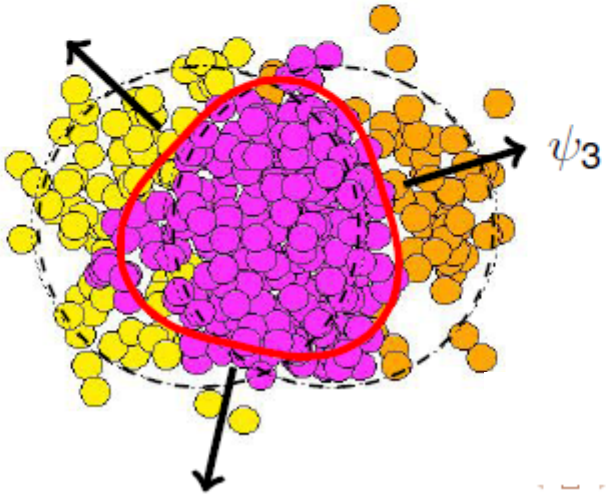

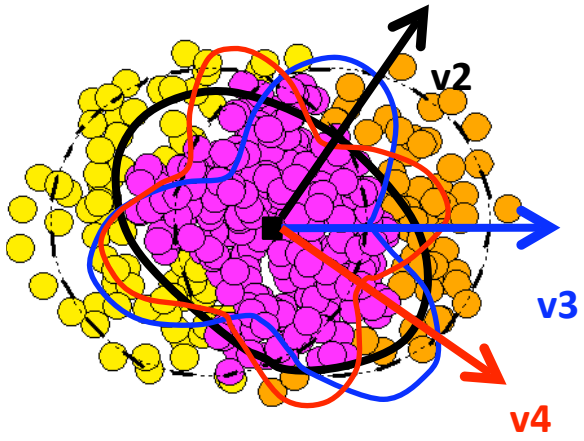

Beam Energy Dependence of v_2, v_3 and v_4

charged particle v_n : $|\eta|<0.35$; reaction plane Φ_n : $|\eta|=1.0\sim2.8$

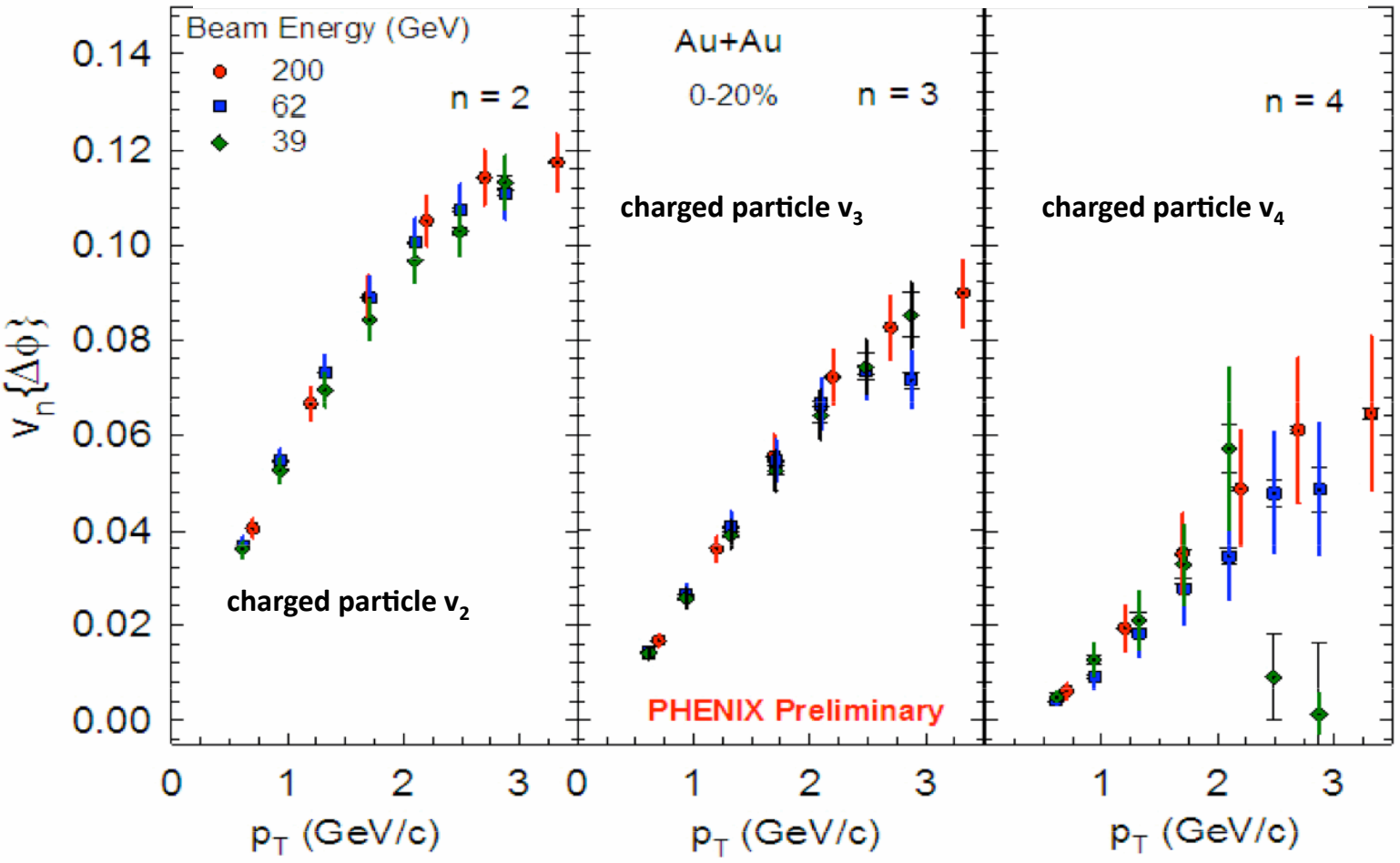

v_2, v_3, v_4 are independent of $\sqrt{s_{NN}}$ for 39, 62.4, 200 GeV

Centrality and p_T-dependences of v_n

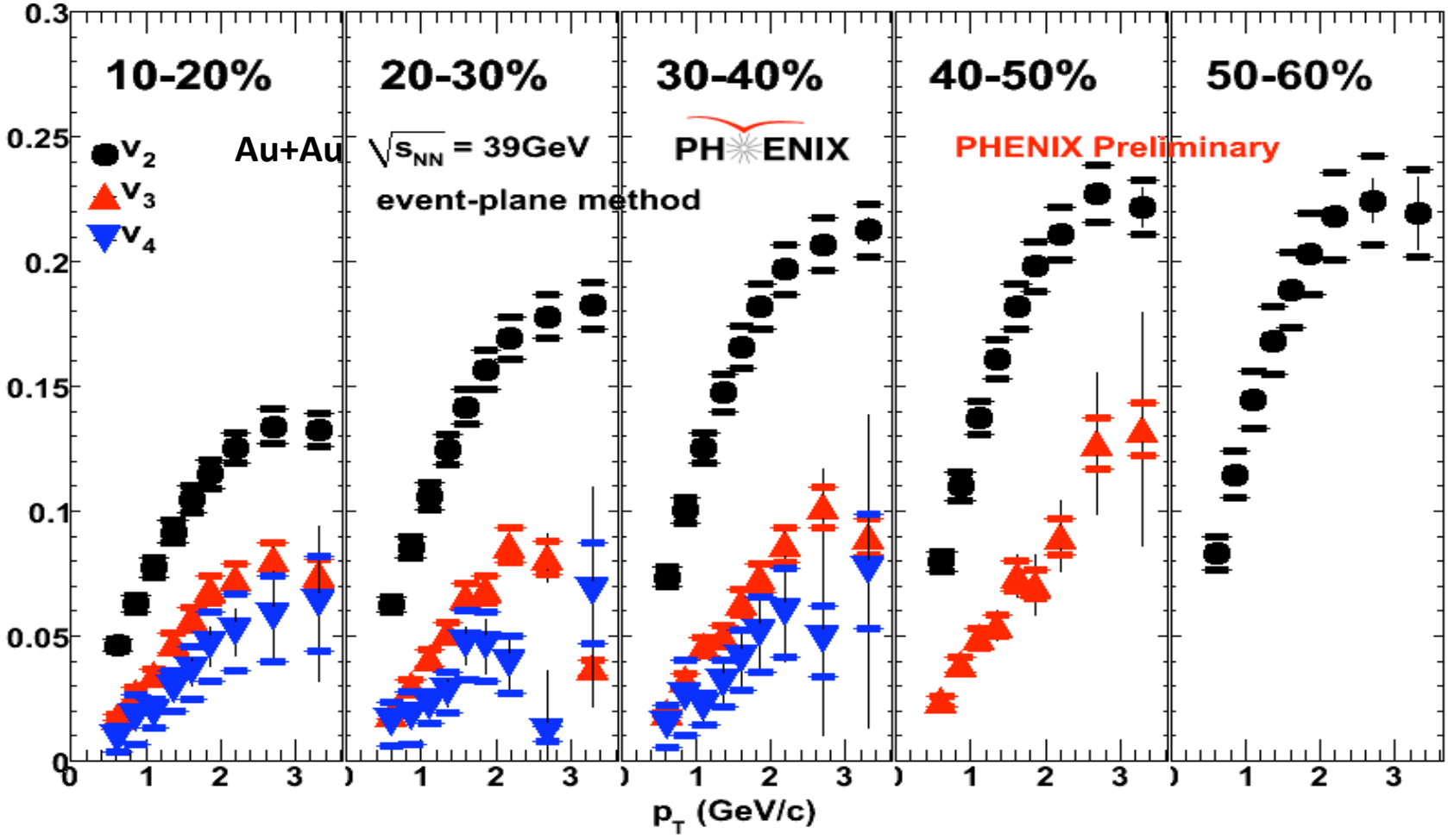

charged particle v_n : $|\eta|<0.35$

reaction plane Φ_n : $|\eta|=1.0\sim2.8$

Centrality and p_T-dependences of v_n

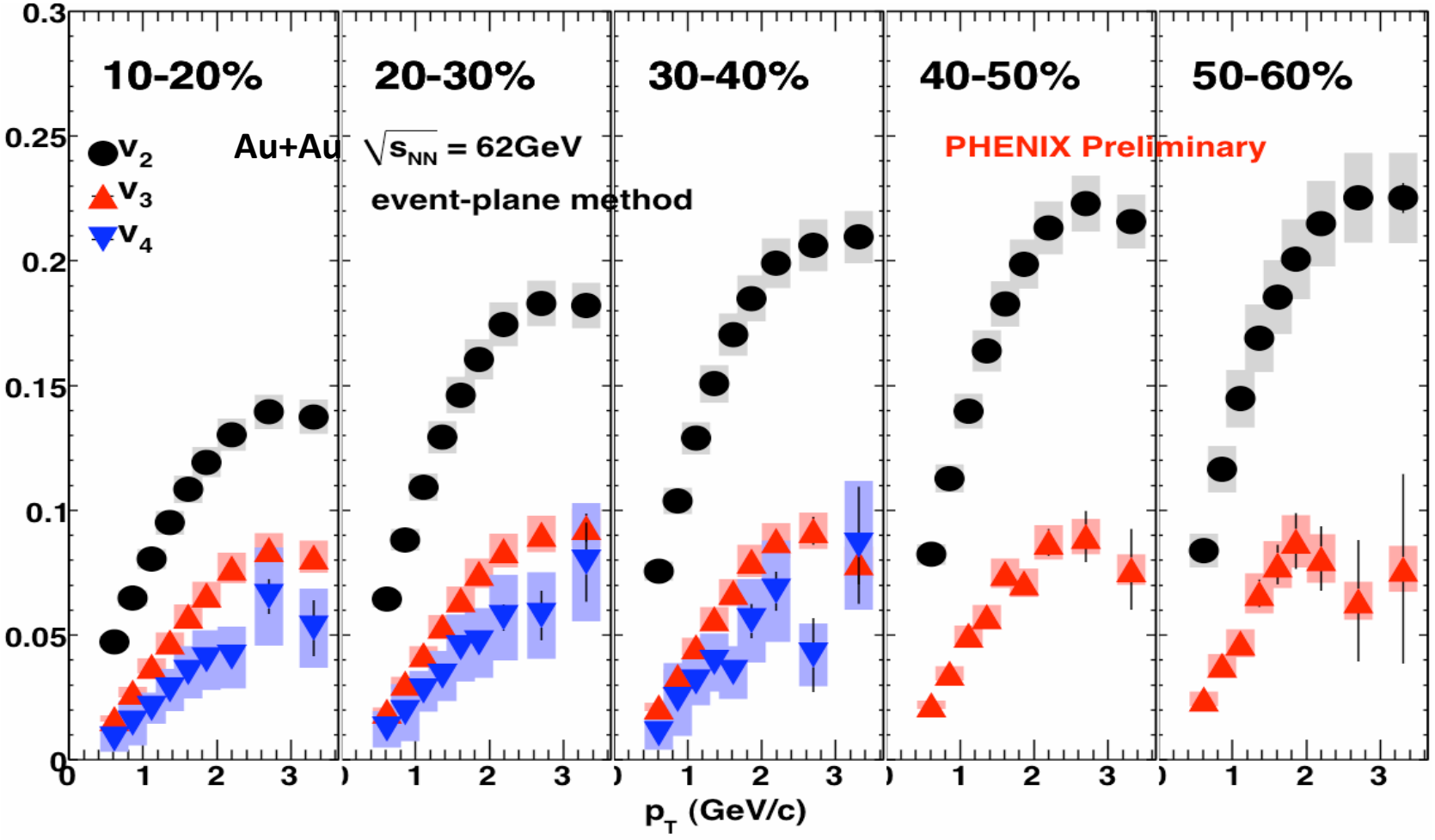

charged particle v_n : $|\eta|<0.35$

reaction plane Φ_n : $|\eta|=1.0\sim2.8$

Centrality and p_T-dependences of v_n

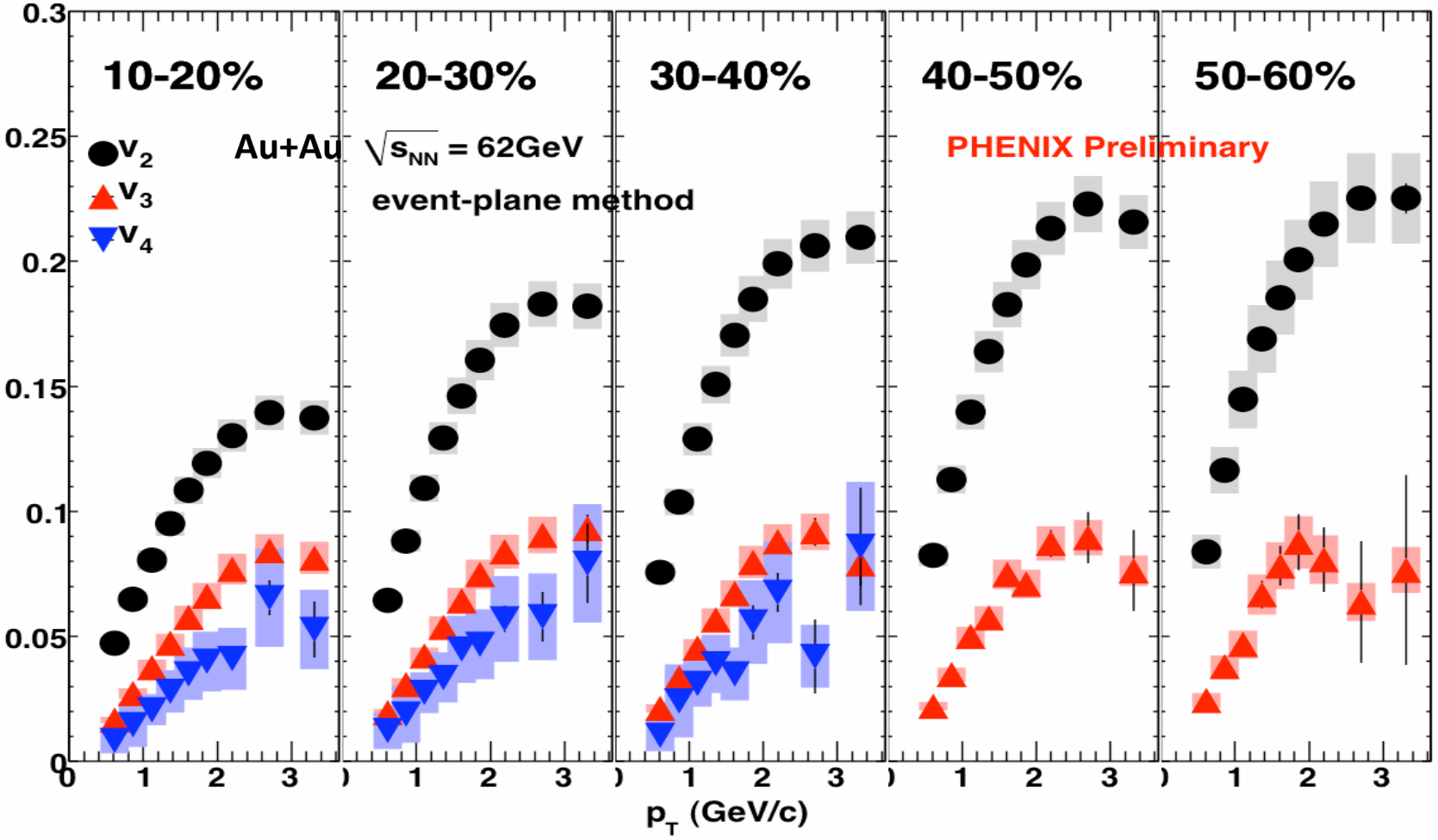

- ✓ Weak centrality dependence of v_3
- ✓ Consistent with initial fluctuation

charged particle v_n : $|\eta|<0.35$
reaction plane Φ_n : $|\eta|=1.0\sim2.8$

Summary

- ★ Results from Beam Energy Scan program provide important constraint on QCD phase diagram. Search for the critical point is ongoing.

- ★ Same flow properties of strongly interacting (de-confined) matter are observed over a wide range of incident energies ($\sqrt{s_{NN}}$=39 GeV - 2.76 TeV).

- ★ Higher order harmonics reveal connection between the anisotropic flow and the fluctuations of the energy density in the initial state.

Backup slides

Required Statistics

	Collision Energies (GeV)	5	7.7	11.5	19.6	27	39	62.4
	Observables	Millions of Events Needed						
Critical Point Signatures	v_2 (up to ~1.5 GeV/c)	**0.3**	**0.2**	**0.1**	**0.1**	**0.1**	**0.1**	
	v_1	0.5	**0.5**	**0.5**	**0.5**	**0.5**	**0.5**	
	Azimuthally sensitive HBT	4	**4**	**3.5**	**3.5**	**3**	**3**	
	PID fluctuations (K/π)	1	**1**	**1**	**1**	**1**	**1**	
	net-proton kurtosis	5	**5**	**5**	**5**	**5**	**5**	
Deconfinement Signatures	n_q scaling π/K/p/Λ $(m_T - m_0)/n$<2GeV	8.5	**6**	**5**	**5**	**4.5**	**4.5**	
	ϕ/Ω up to p_T/n_q=2 GeV/c		56	25	**18**	**13**	**12**	
	R_{CP} up to p_T ~4.5 GeV/c (at 17.3) 5.5 (at 27) & 6 GeV/c (at 39)				**15**	**33**	**24**	
	Total Number of Events Taken	0	**5**	**11**	**17**	**13(**	**17(**	**17(**

Maximum Net Baryon Density

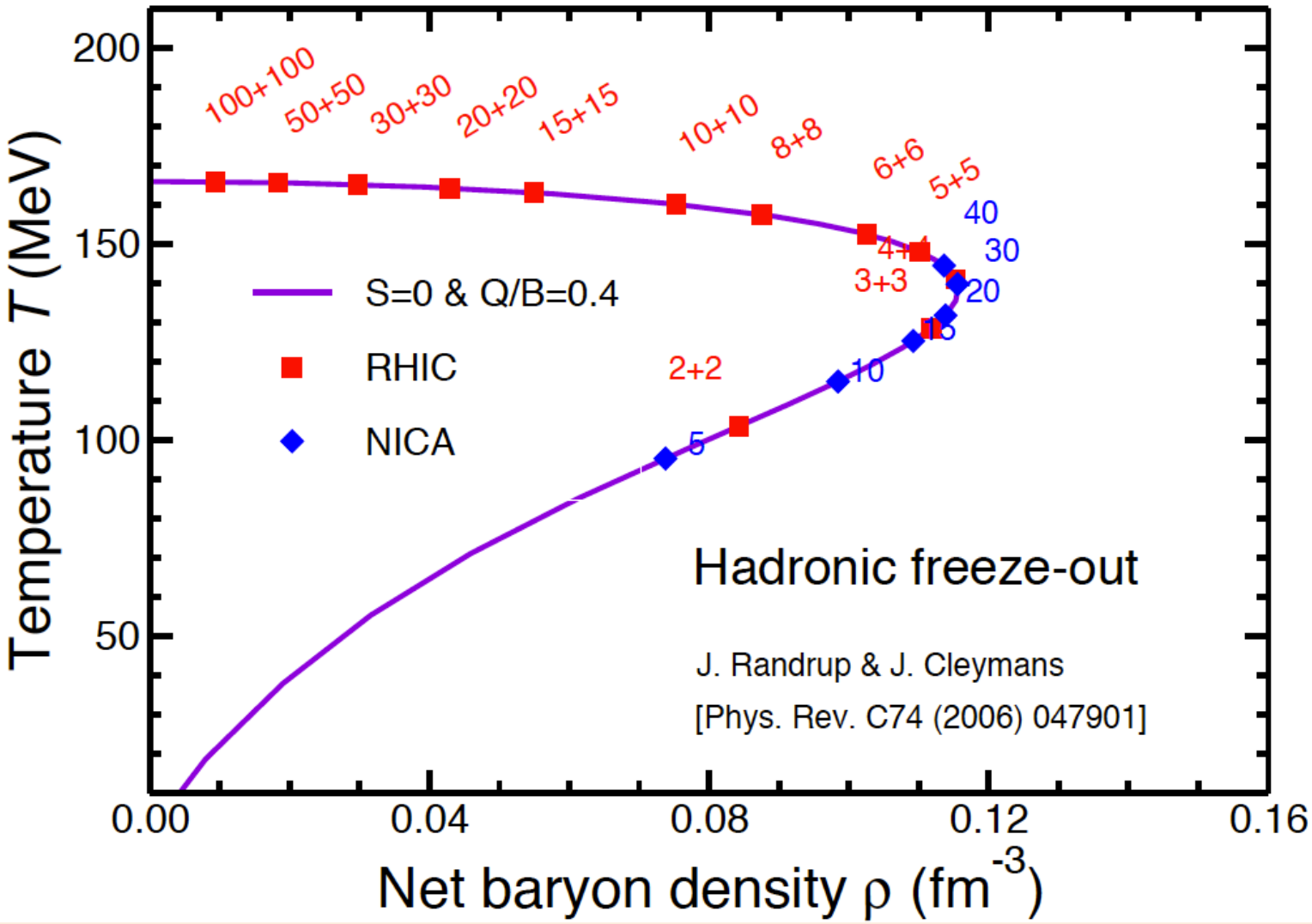

The maximum baryon density at freeze-out expected for $\sqrt{s_{NN}} \approx 6\text{-}8$ GeV

Maximum Net Baryon Density

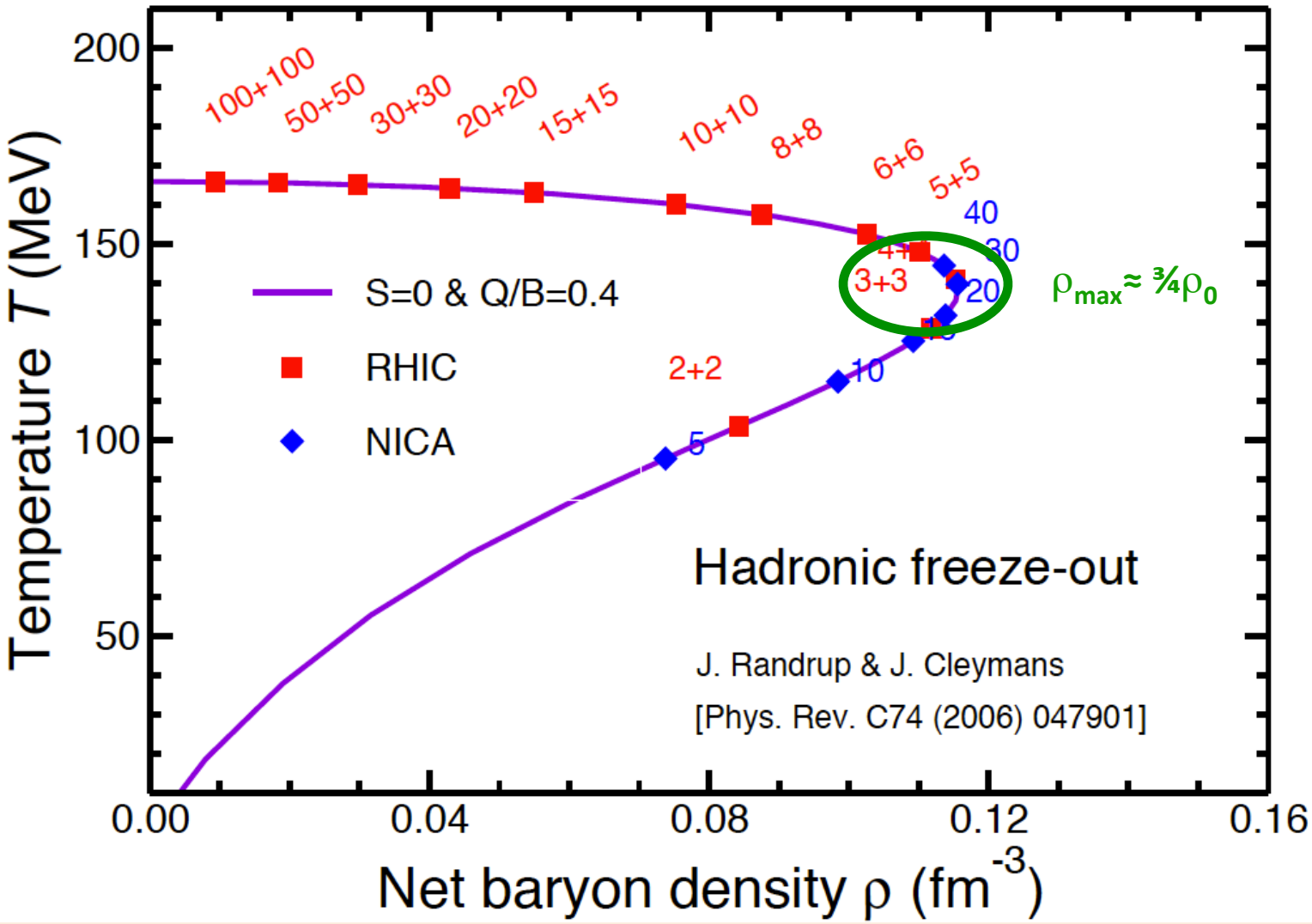

The maximum baryon density at freeze-out expected for $\sqrt{s_{NN}} \approx 6\text{-}8$ GeV

Directed Flow

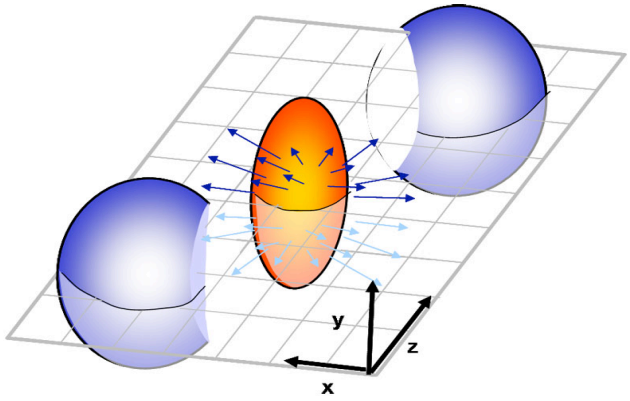

$$\frac{dN}{d\varphi} \propto \left(1 + 2\sum_{n=1}^{+\infty} v_n \cos\left[n(\varphi - \psi_n)\right]\right)$$

Directed flow is quantified by the first harmonic: $v_1 = \langle \cos(\phi - \Psi_r) \rangle$

$$\phi = \tan^{-1}\left(\frac{p_x}{p_y}\right)$$

- Directed flow is due to the sideward motion of the particles within the reaction plane.
- Generated already during the nuclear passage time ($2R/\gamma \approx .1$ fm/c@200GeV)

⇒ It probes the onset of bulk collective dynamics during thermalization (preequilibrium)

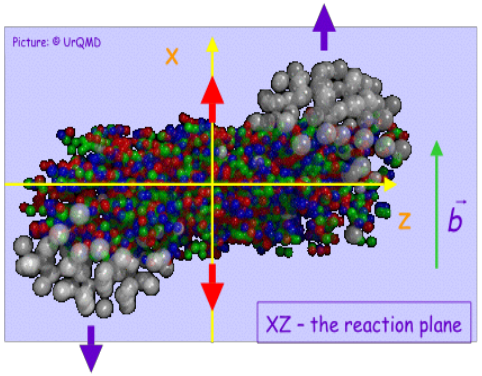

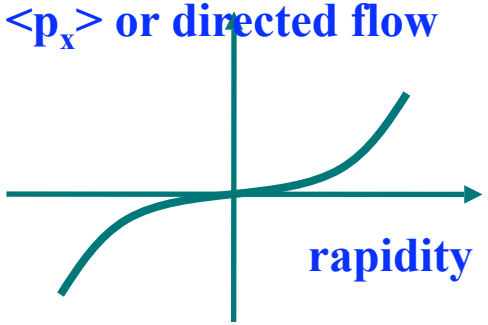

$v_1(y)$ is sensitive to baryon transport, space - momentum correlations and QGP formation

BES v_2: Particles vs. Anti-particles

STAR AuAu@62.4: Phys.Rev.C75, 054906 (2007)

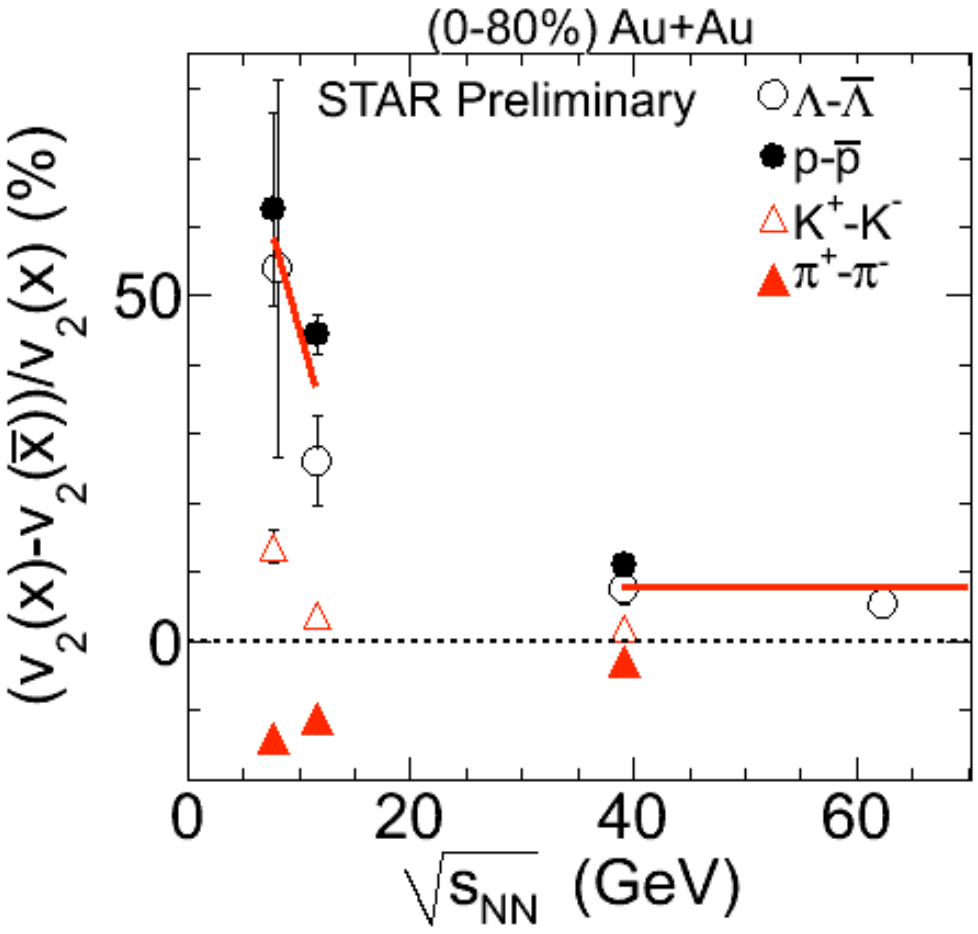

For Beam energy ≥ 39 GeV:

- Baryon and anti-baryon v_2 are consistent within 10%
- Almost no difference for meson v_2

Beam energy = 7.7, 11.5 GeV:

- Significant difference of baryon and anti-baryon v_2

→ *Increasing with decrease of beam energy*

- $v_2(K^+) > v_2(K^-)$ at 7.7 GeV
- $v_2(\pi^-) > v_2(\pi^+)$ at 7.7, 11.5 GeV

Possible explanation:

- Baryon transport to mid-rapidity
- Absorption in hadronic environment

The difference between particles and anti-particles is observed

Reaction plane resolution of n^{th} order plane

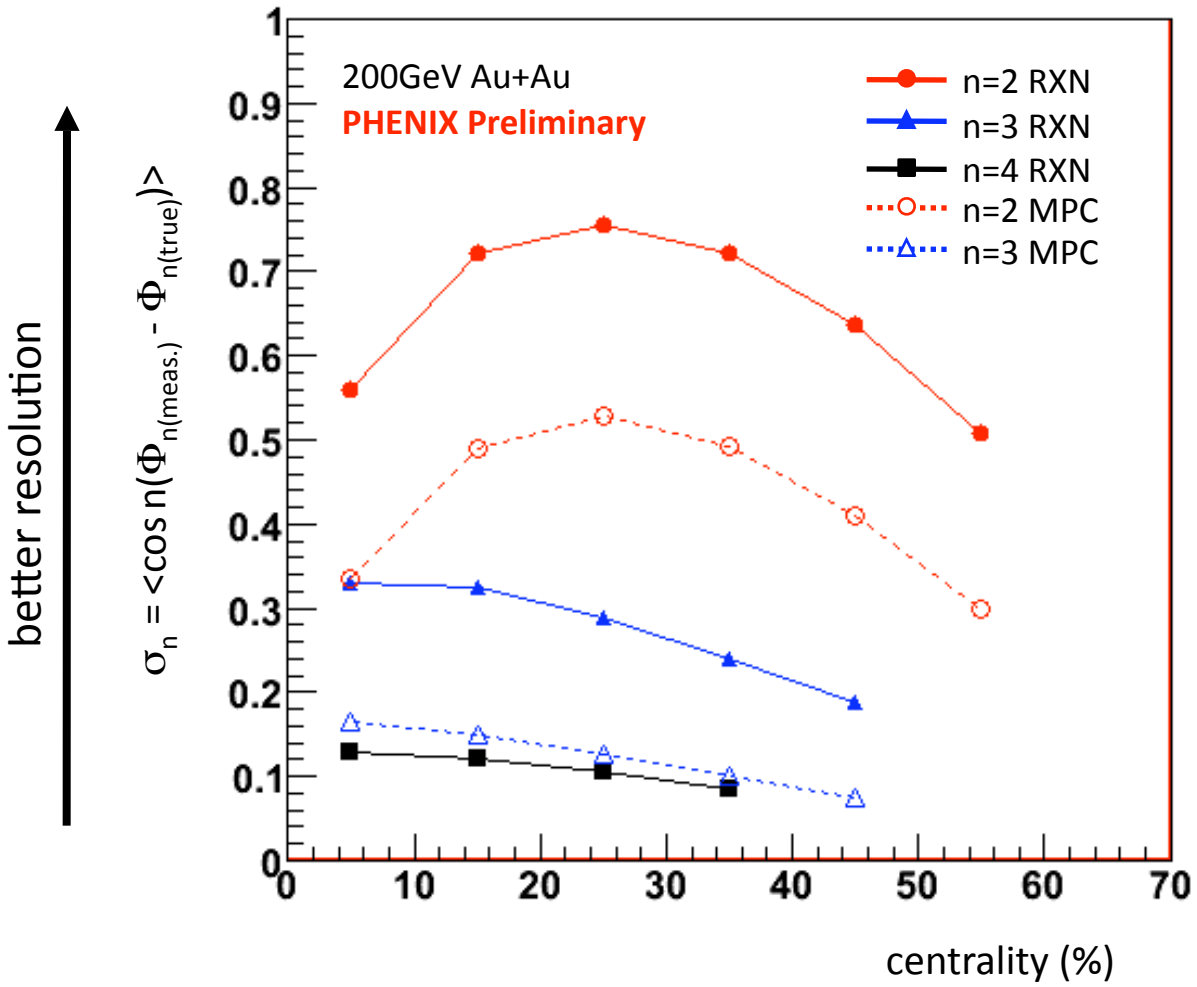

RXN $|\eta| = 1.0 \sim 2.8$
MPC $|\eta| = 3.1 \sim 3.7$

positive correlation in Φ_3 between opposite η up to +/– 3 ~ 4

No sign flipping in Φ_3 observed

--> Initial geometrical fluctuation

n_q-scaling of v_3

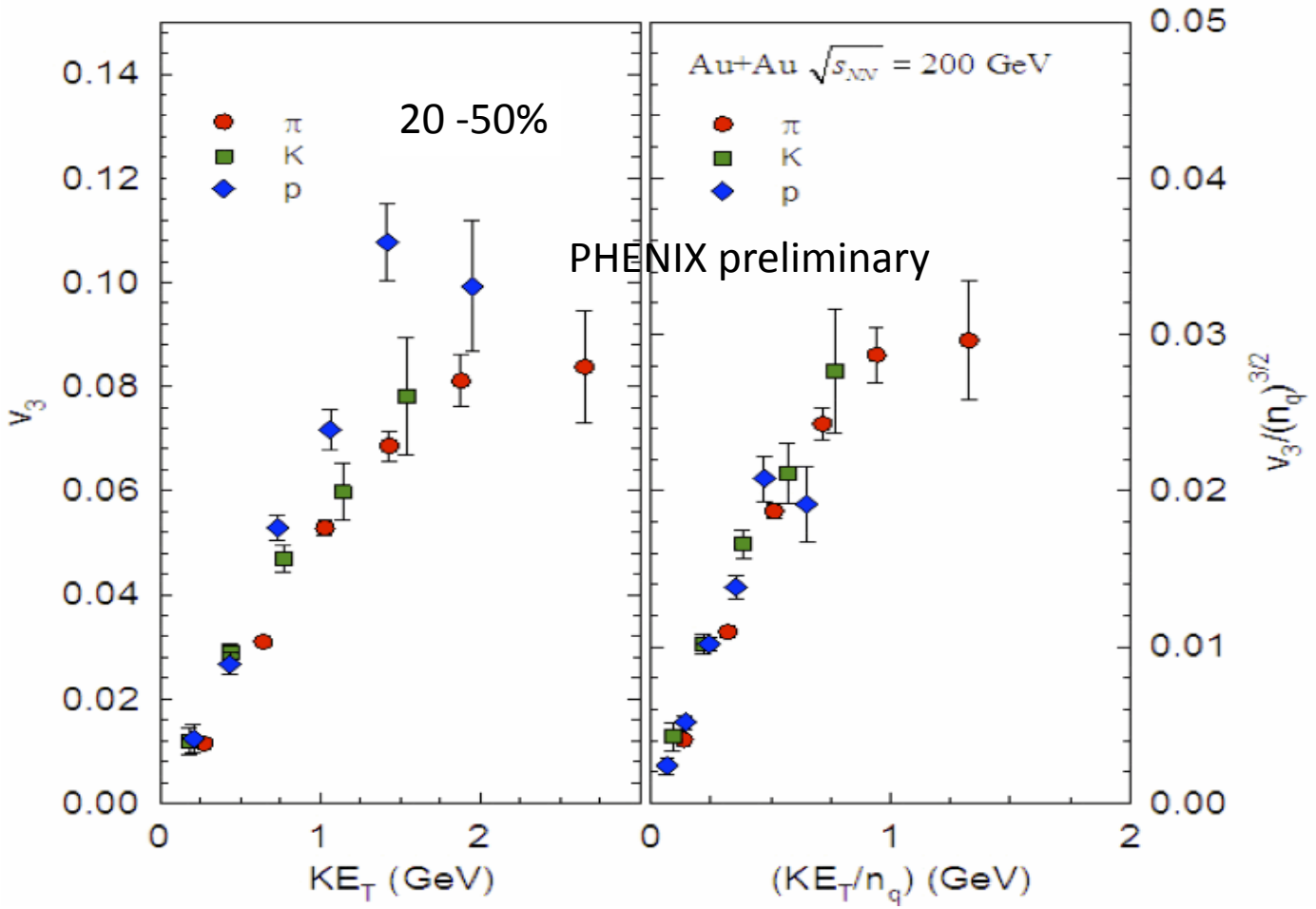

- Like v_2, constituent quark scaling is seen with v_3.
- Evidence of partonic flow.

The Horn and Other Yields

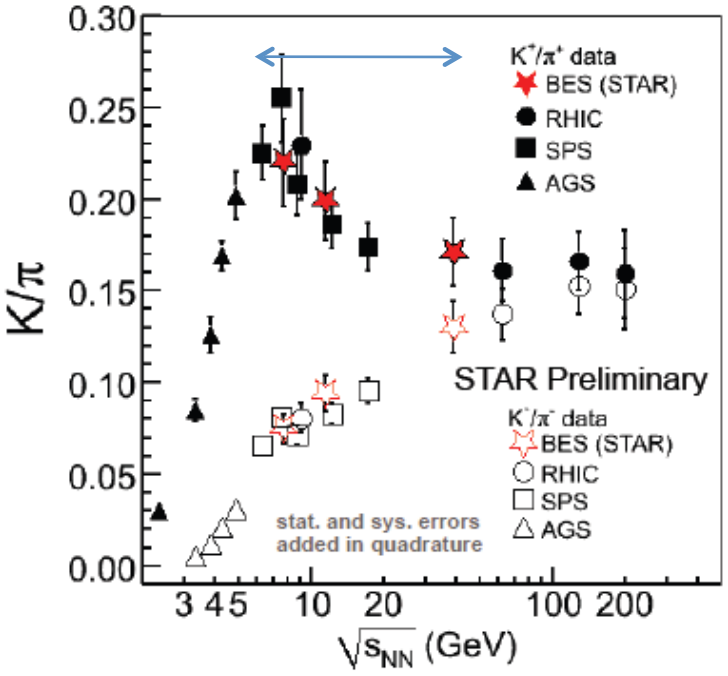

STAR Ref.: B. I. Abelev et al., PRC79 (2009) 034909
B. I. Abelev et al., PRC81 (2010) 024911

E802 Ref.: L. Ahle et al., PRC58 (1998) 3523
L. Ahle et al., PRC80 (1999) 044904
E895 Ref.: J. L. Klay et al., PRC68 (2003) 054905
E877 Ref.: J. Barrette et al., PRC62 (2000) 024901

NA49 Ref.: S. V. Afanasiev et al., PRC66 (2002) 054902
C. Alt et al., PRC77 (2008) 024903

The Horn and Other Yields

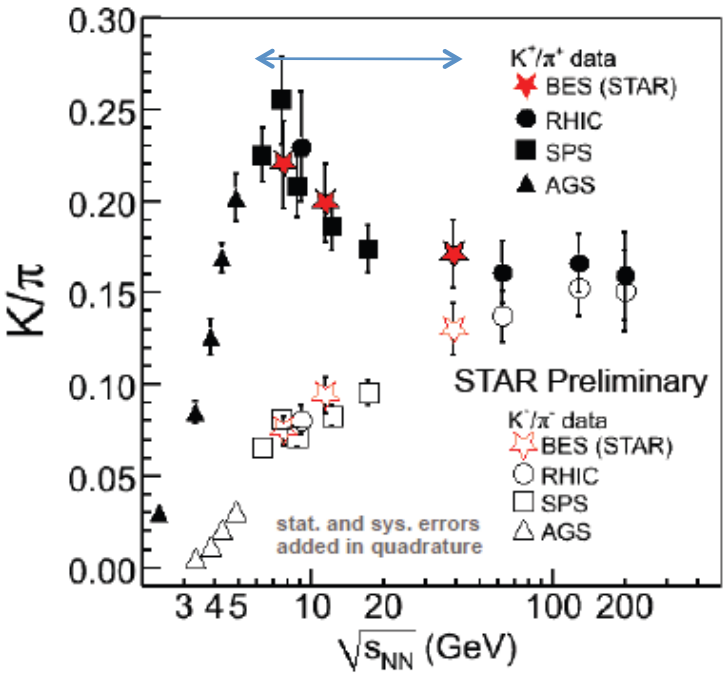

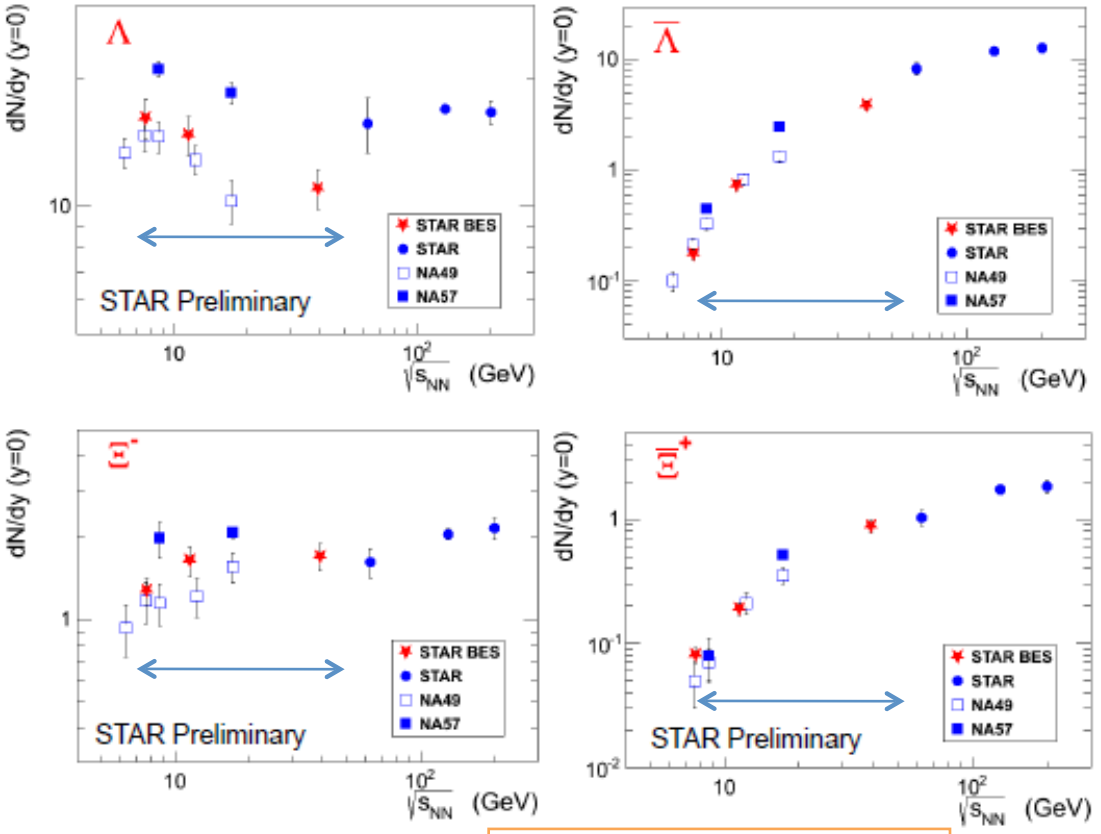

STAR Ref.: B. I. Abelev et al., PRC79 (2009) 034909
B. I. Abelev et al., PRC81 (2010) 024911

E802 Ref.: L. Ahle et al., PRC58 (1998) 3523
L. Ahle et al., PRC80 (1999) 044904
E895 Ref.: J. L. Klay et al., PRC68 (2003) 054905
E877 Ref.: J. Barrette et al., PRC62 (2000) 024901

NA49 Ref.: S. V. Afanasiev et al., PRC66 (2002) 054902
C. Alt et al., PRC77 (2008) 024903

NA49, PRC78,034918.
NA57, PLB595,68; JPG32, 427
STAR, PRL86,89,92,98;PRC83

The Horn and Other Yields

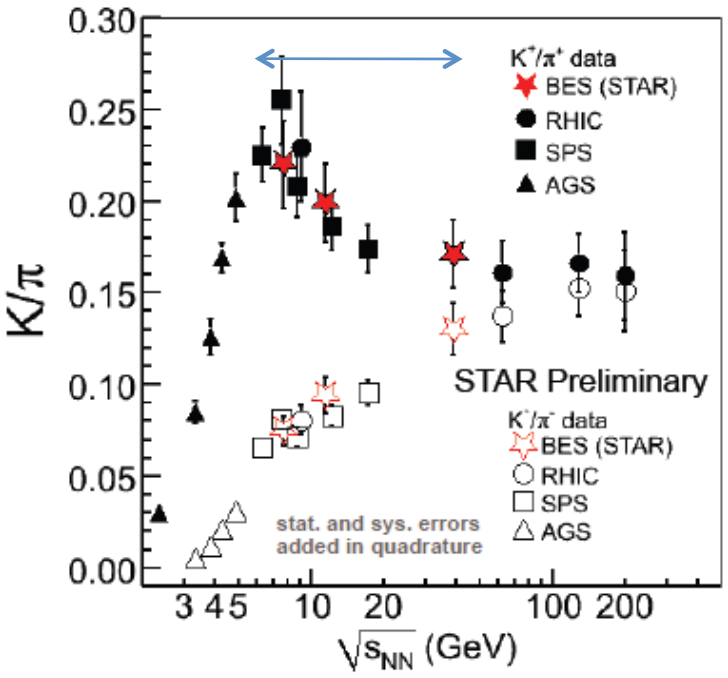

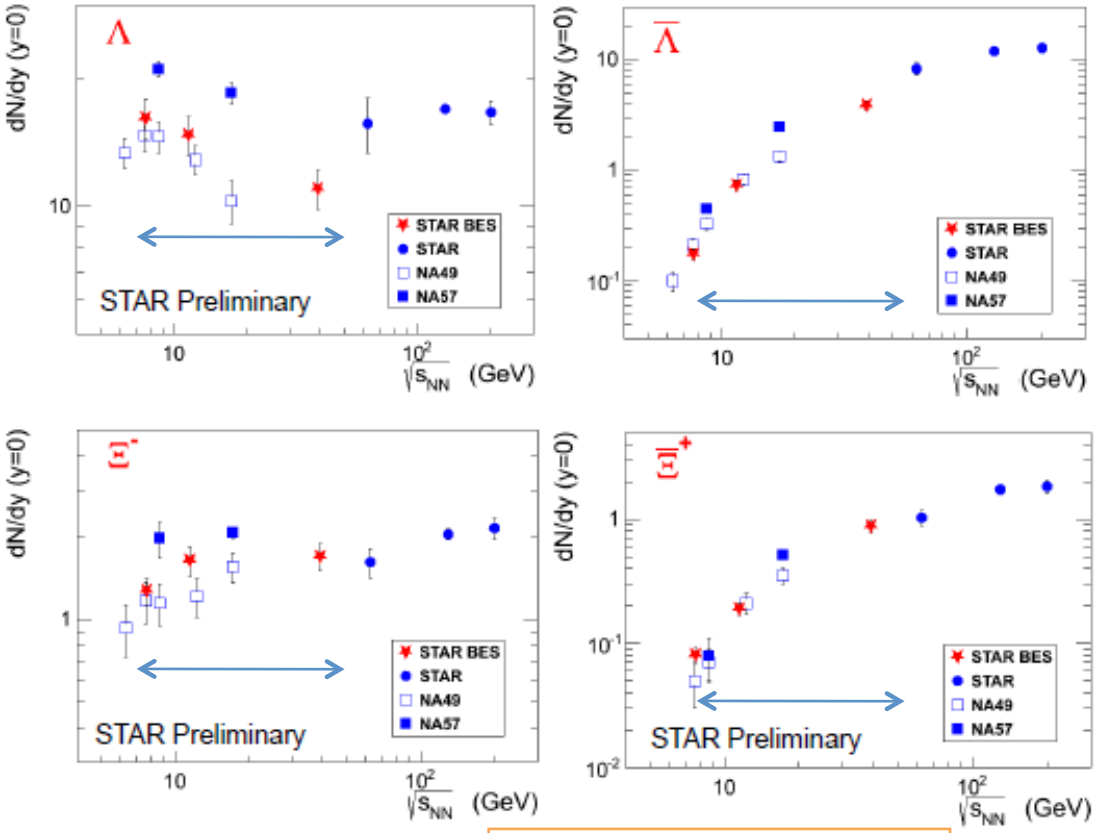

STAR Ref.: B. I. Abelev et al., PRC79 (2009) 034909
B. I. Abelev et al., PRC81 (2010) 024911

E802 Ref.: L. Ahle et al., PRC58 (1998) 3523
L. Ahle et al., PRC80 (1999) 044904
E895 Ref.: J. L. Klay et al., PRC68 (2003) 054905
E877 Ref.: J. Barrette et al., PRC62 (2000) 024901

NA49 Ref.: S. V. Afanasiev et al., PRC66 (2002) 054902
C. Alt et al., PRC77 (2008) 024903

The STAR BES data are consistent with the NA49 results

NA49, PRC78,034918.
NA57, PLB595,68; JPG32, 427
STAR, PRL86,89,92,98;PRC83

v_3 and initial fluctuation

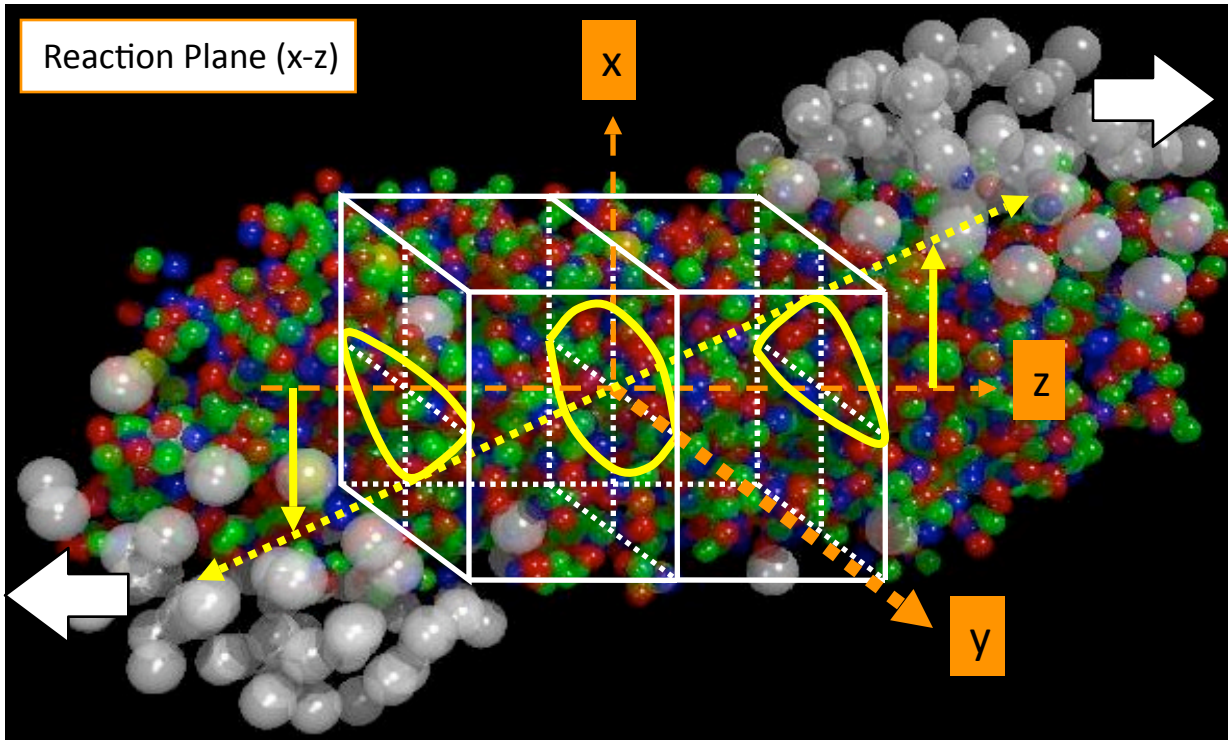

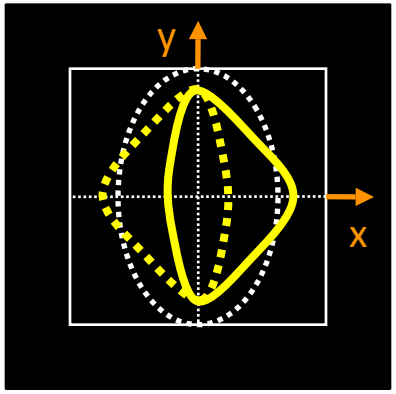

arXiv:1003.0194

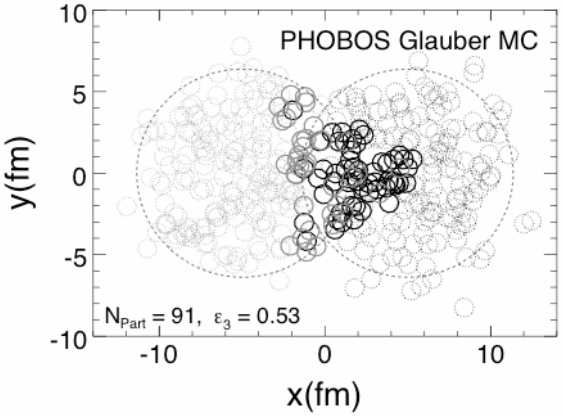

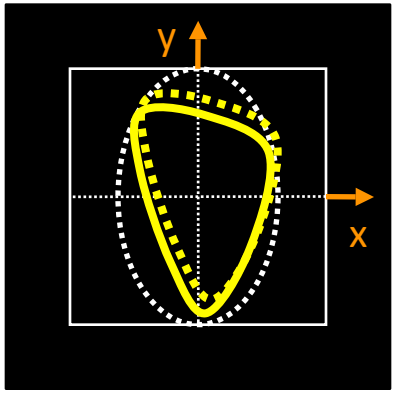

black-disk --> sign-flipping v_3

initial fluctuation --> no-sign-flipping v_3

Indication of strong non-flipping and weak sign-flipping v_3